ON THE SELECTION OF COMMERCIALLY AVAILABLE SN-AG-CU PB-FREE BALLS COMPONENTS OVER RE-BALLING THE COMPONENTS WITH SN37PB BALLS TO COMPLY WITH THE RESTRICTION OF HAZARDOUS SUBSTANCES DIRECTIVE IN THE AEROSPACE INDUSTRY

by

Lorraine M. Renta Rosa

A thesis submitted in partial fulfillment of the requirements for the degree of

MASTER OF SCIENCE
in
MECHANICAL ENGINEERING

UNIVERSITY OF PUERTO RICO
MAYAGÜEZ CAMPUS
2009

Approved by:

_____	_____
Pedro Quintero, Ph.D. Member, Graduate Committee	Date
_____	_____
Pablo Cáceres, Ph.D. Member, Graduate Committee	Date
_____	_____
Ricky Valentín, Ph.D. President, Graduate Committee	Date
_____	_____
David González, Ph.D. Representative of Graduate Studies	Date
_____	_____
José Colucci, Ph.D. Representative of ME Director	Date

ABSTRACT

A modeling approach based on physics of failure is presented that quantifies the interactions between different thermal cycles applied to Ball Grid Arrays (BGA). The approach is formulated at the microscale, incorporating physical mechanisms of intermetallics, and at the macroscale, capturing the creep phenomenon as dominant failure driver. The prediction trends agree with experimental results, confirming that the dominant damage switches have been captured in the Finite Element Models. Both macroscale and microscale damage models are applied to predict the durability of two BGA structures: backward compatible SAC balls soldered to eutectic SnPb paste, and re-balled eutectic SnPb balls soldered to eutectic SnPb paste. Results show that re-balled cases have higher inelastic energy density per cycle averaged over damage volume. Results also show that the inelastic energy density is higher across the bulk of the improperly mixed backward compatible solder balls when compared to properly mixed backward compatible solder balls.

RESUMEN

Se presenta un enfoque de modelaje basado en física de falla que cuantifica interacciones entre diferentes ciclos termales aplicados a Matrices de Rejilla de Bolas (BGA). El enfoque es formulado en modelos a microescala, incorporando mecanismos físicos de intermetálicos, y macroescala, capturando el pandeo como gestor dominante de falla. Tendencias de predicción concuerdan con resultados experimentales, confirmando que parámetros de daño dominantes se han capturado en los Modelos de Elementos Finitos. Ambos modelos son aplicados para predecir la durabilidad de dos estructuras BGA: bolas de compatibilidad descendente SAC soldadas en pasta SnPb eutéctica, y bolas re-ensambladas de SnPb eutéctico soldadas en pasta SnPb eutéctica. Resultados muestran que casos re-ensamblados tienen densidad de energía por ciclo promediada sobre volumen dañado mayores. También muestran que densidad de energía inelástica es mayor en el grueso de las bolas de soldaduras de compatibilidad descendente no-mezcladas comparadas con bolas de soldaduras de compatibilidad descendente mezcladas.

For Ma, Pa and Lou

ACKNOWLEDGEMENTS

Several people have collaborated with me during my graduate studies in the Mechanical Engineering Department at the University of Puerto Rico, Mayagüez Campus. I begin by acknowledging the great opportunity given to me by Dr. Ricky Valentín, my advisor, to carry out research under his supervision. I acknowledge Dr. Pedro Quintero for his encouragement and words of advice throughout the process. I would also like to acknowledge Dr. Pablo Cáceres for his support and Dr. Francisco Rodríguez for his guidance. I owe special thanks to Dr. Frederick Just for inspiring me throughout my years as a student. To them I am indebted.

Finally, I sincerely thank my family. Their unconditional support, inspiration and words of encouragement have made the difference throughout this process. To Ma, Pa, Lou and Carlos I give my thanks.

LIST OF CONTENTS

LIST OF TABLES

LIST OF FIGURES

LIST OF SYMBOLS AND ABBREVIATIONS

2-D	Two dimensions / Two dimensional
3-D	Three dimensions / Three dimensional
Ag	Silver
ATC	Accelerated thermal cycling
ATSDR	Agency for Toxic Substances and Disease Registry
BGA	Ball grid array
CERCLA	Comprehensive Environmental Response, Compensation, and Liability Act
CSP	Chip scale package
Cu	Copper
DHHS	Department of Health and Human Services
EPA	Environmental Protection Agency
EU	European Union
FEA	Finite element analysis

FEM	Finite element modeling
Pb	Lead
Pb-free	Lead-free
PCB	Printed circuit board
PoF	Physics of failure
PWB	Printed wiring board
RB	Re-balled
RoHS	Restriction of Hazardous Substances
SAC	Tin-Silver-Copper alloy, common abbreviation in industry
Sn	Tin
SnAgCu	Tin-Silver-Copper alloy
SnPb	Tin-Lead alloy
Sn37Pb	Eutectic tin-lead alloy
US	United States
WEEE	Waste of Electrical and Electronic Equipment

1 INTRODUCTION

Lead (Pb) is a naturally occurring metal found in small amounts in the earth's crust. It can be found in many places within our environment, either naturally or as a byproduct of human activity. Exposure to Pb may cause a range of negative health effects to people, from behavioral problems and learning disabilities, to seizures and death.[1] The use of Pb in human activities has been dramatically reduced in recent years due to the health hazard it poses to people. Legislation worldwide is contributing to the push toward the gradual elimination of Pb in manufacturing processes.[2]

Much of the Pb found in our surroundings comes from human activities including burning fossil fuels, mining, and manufacturing of batteries, ammunition, and devices to shield X-rays. Metal products and solders have traditionally included Pb, and solders used in the electronics industry are not the exception.[3] Legislation that pushes for the elimination of Pb and other toxic substances from manufacturing practices has included

the elimination of Pb in metal alloys used in solders. This has led the scientific community to study the effectiveness and reliability of a new breed of Pb-free solders for a wide range of applications.

The aerospace industry is one of many global industries faced with the challenge of eliminating Pb from its electronic products. The present work focuses on the issue of reliability of Pb-free solder for aerospace applications. Specifically, it makes emphasis on the benefits and disadvantages of several approaches that may be taken in order to eliminate leaded solder from aerospace electronics. This will allow the aerospace industry to comply with legislation and have a positive influence on the environment.

1.1 MOTIVATION

Products placed in the European market must comply with the Restriction of Hazardous Substances directive (RoHS) as of July 1, 2006.[4] This states that products should not contain excessive amounts of certain substances harmful to the environment, among them, Pb. Manufacturers worldwide have altered their processes to comply with this standard in order to sell their products in the European Union. This has made Pb-free products more abundant in the global electronics supply chain. The aerospace industry is a relatively small electronics consumer among the various global industries that procures its components from the Pb-free rich global supply chain; thus it is being forced to transition toward the use of the Pb-free components available.[5]

The aerospace industry manufactures products that have unique operating environments including extreme temperatures, shock levels and vibrations. Product reliability in this industry is of utmost importance and attention is being given to the transition into Pb-free electronics assembly. Performance implications are being identified through research and results are sometimes conflicting. No data is available for long-term reliability, limiting the full incorporation of the Pb-free components. Currently there is not a single preferred Pb-free substitute for all products and applications, including commonly used electronic packages such as the ball grid array.

When discussing ball grid array/chip scale package (BGA/CSP) we refer to backward compatibility when components are attached to the printed circuit board (PCB) using Pb-free balls and tin-lead (SnPb) solder paste.[6] In general, studies have shown conflicting results when testing the reliability of backward compatible BGA/CSP assemblies in comparison to SnPb ball/SnPb paste and SnAgCu ball/SnAgCu paste control assemblies under accelerated thermal cycling (ATC).[7 8]

The lack of reliable data to support the safe use of SAC alloys for electronics in aerospace applications has led manufacturers to re-ball their components. In this process, SAC balls are removed and replaced with eutectic SnPb for soldering. This gives manufacturers a greater sense of security in comparison to soldering with Pb-free balls. Yet it is worth noting that this process can foment the formation of intermetallics between the SnPb solder and the Pb-free ball remnants, causing yet another reliability issue.

This work will model two common assembly scenarios while taking into consideration the intermetallics formed. These scenarios are: a) backward compatible assembly, with Pb-free solder ball and SnPb paste and b) re-balled assembly, with SnPb solder ball and SnPb solder paste with Pb-free residuals.

This is an approach that has not been taken before in the study of this important subject. It will bring forward the risk associated with intermetallics in the study of Pb-free solder reliability.

1.2 OBJECTIVES AND TASKS

The primary objective of this study is to research the viability and limitations associated with using lead-free solders in ball grid array assemblies versus removing Pb-free solder from the assemblies and re-balling them with SnPb solder. This will be done taking into consideration the intermetallics formed in each of the different assemblies and the mixing of different solder alloys. Finite element modeling will be the primary tool used in this study for the reliability assessment.

The specific objectives include:

1. Model various BGA assembly geometries using finite element modeling.
2. Model thermal cycling tests on the assemblies.

3. Evaluate and compare energy density results.
4. Reach conclusions on the viability and limitations associated with using Pb-free solders in ball grid array assemblies versus removing Pb-free solder from the assemblies and re-balling them with SnPb solder.

1.3 CONTRIBUTION OF THIS RESEARCH

This work will model several assembly scenarios under ATC while taking into consideration the intermetallics formed during these different scenarios. This is an approach that has not been taken before in the study of this important subject. It will bring forward the importance of considering intermetallics in the study of Pb-free solder reliability in BGAs.

Experiments taking the effects of BGA re-balling into account have not been found to exist. In much the same way, finite element modeling considering the effects of Pb-free solder remnants on BGA Cu pads after re-balling have not been found to exist either. These Cu remnants give rise to new possible intermetallics that have not been taken into account in any experiment or FEA found to date. Comparison of the subsequent results of ATC tests in this case with experimental data has therefore not been found to exist either.

2 LITERATURE REVIEW

Many experiments and finite element models have studied the reliability of solders, including SnPb solders. Recent restrictions on the use of leaded solders have pushed for the study of Pb-free solders in different configurations and operating environments. Experiments taking the effects of re-balling into account have not been found in the literature. In much the same way, finite element models considering the effects of re-balling have not been found in the literature either. Pb-free solder remnants on Cu pads give rise to new possible intermetallics that have not been taken into account in any experiment or FEA found to date. Comparison of the subsequent results of ATC tests in this case with experimental data has therefore not been found in the literature. Below is a review of literature stating the prior art on the subject that serves as a background for this study.

There are four major ways in which soldering BGAs can take place. These are SnPb soldering, Pb-free soldering, forward compatible soldering and backward

compatible soldering. SnPb soldering has SnPb solder paste and solder balls. Pb-free soldering has Pb-free solder paste and solder balls. Forward compatible soldering has Pb-free paste and SnPb solder balls. Backward compatible soldering has SnPb paste and Pb-free solder balls. In this study the soldering configurations of interest are SnPb soldering, Pb-free soldering and backward compatible soldering.

ATC has been widely accepted as a method to assess the reliability of SnPb solders for decades. During these tests, solder joints develop changing compositions, stress and microstructural states which vary spatially throughout the solder joint. This varies with changes in the number of thermal cycles per test as well as with different temperature ranges. The recent shift to Pb-free solder has brought to the light the limitations of this test method. ATC tests with Pb-free solders show repeatability, yet they do not show the same degree of reliable results as tests done with the traditional SnPb solder.[9] This is mainly because ATC for Pb-free solders have proved to depend on the particular material properties of the solder under test.

Consumer applications have an advantage over other extreme applications in that the consequences of malfunction do not generally pose great threats to life or property. More specifically, general commercial markets that focus on domestic goods and electronics need not worry about the reliability of their solders in extreme temperatures, vibrations scenarios, or wide temperature swings. In any case, when a domestic product malfunctions the main consequence is that the end of its life has been reached and a consumer can readily fix the damage or acquire a new product. When considering

products not aimed to the general commercial consumer market these advantages are not necessarily present.

The products developed by the aerospace industry necessarily need to be reliable. These products generally undergo temperature cycling, operate in extremely hot or cold temperatures and suffer vibration. Scientists and engineers have recognized that substituting the eutectic SnPb solder used to date with a Pb-free solder is not to be taken lightly. This has promoted the existence of several experimental studies that test the reliability of Pb-free solder joints for applications related to aerospace conditions. ATC tests are a starting point for these studies as more and more information is being learned about the Pb-free solders under study.

Studies have been conducted to test the reliability of backward compatible BGA soldering under different ATC conditions. These studies consistently show conflicting results. This is primarily due to the lack of regulations governing the study parameters and the subsequent large variation in test conditions. There are two experimental studies that have had similar test conditions, making them suitable for comparison within the range of studies conducted on the subject. Both studies are considered to be leaders, or benchmarks, in the study of Pb-free solder reliability. As with many other tests, they show conflicting results. These conflicting results bring more attention to the fact that accurate, consistent data on Pb-free solder reliability is non-existent.

The first of the studies aforementioned was conducted by Bath, et al. in 2005.[7] In this study a backward compatible BGA/CSP assembly was subjected to ATC. The thermal cycle ranged from 0°C to 100°C. The results based on cycles to failure showed that the reliability of the backward compatible BGA/CSP assembly under this ATC test was poorer than the SnPb soldered assembly and the Pb-free soldered assembly that were used as experimental controls. Table 2-1 shows a summary of these results.

Table 2-1 Summary of Results of Experimental Study by Bath, et al.

Temperature Range (°C)	Backward Compatible Assembly	SnPb Assembly	Pb-free Assembly
0 to 100	Baseline	Better than baseline	Better than baseline

The second of the studies discussed was conducted by Nandagopal, et al. in 2005.[8] In this study two ATC tests were performed on backward compatible BGA/CSP assemblies. The first thermal cycle ranged from 0°C to 100°C ATC, just as the cycle run by Bath, et al. previously described. Results showed greater reliability for the backward compatible BGA/CSP assembly in comparison to the SnPb soldered assembly. They also showed poorer reliability for the backward compatible BGA/CSP assembly in comparison to the Pb-free soldered assembly. The second thermal cycle had a temperature range from -40°C to 125°C. In this case, backward compatible BGA/CSP assembly showed greater reliability than the SnPb soldered assembly and the Pb-free soldered assembly. Table 2-2 shows a summary of the results of this experiment.

Table 2-2 Summary of Results of Experimental Study by Nandagopal, et al.

Temperature Range (°C)	Backward Compatible Assembly	SnPb Assembly	Pb-free Assembly
0 to 100	Baseline	Poorer than baseline	Better than baseline
-40 to 125	Baseline	Poorer than baseline	Poorer than baseline

Finite element modeling (FEM) has also been used to study the reliability of backward compatible soldering and Pb-free soldering. This allows the study of physical phenomena without the need of constant experimental procedures, potentially reducing costs for a research firm or corporation. Models are used to predict physical response and are the result of reducing physical phenomena to mathematical relations that correspond to parameters representing these phenomena. The behavior of the materials under study is mathematically described and appropriate initial and boundary conditions must be applied.[10]

Vandevelde, et al. conducted studies using FEM.[11] The ATC used were the same as those used by Nandagopal, et al. in their experimental tests. The authors considered two FEM outputs, inelastic energy density and inelastic strain. Upon considering both analysis methods the results proved to be conflicting, prompting the authors to recommend that experimental results should be used to determine whether strain or energy density should be selected as the damage parameter to determine reliability. The conflicting results could have been attributed to the lack of faithful modeling of the solder assemblies, i.e., the lack of consideration of intermetallics in the solder ball structure.

These intermetallics are formed between the different elements found in each of the assemblies and have not been considered by Vandevelde or other finite element modeling tests.

Zhang, et al. also conducted FEM. The damage criteria used were inelastic strain range and work density.[12] ATC tested included the two previously described with modifications in ramp rate and dwell time. Just as the Vandevelde, et al. conclusion, Zhang suggests that the use of inelastic strain range as damage criterion be closely examined as results using work density as damage criterion proved to correlate with experimental results better than results using strain range.

These studies serve as a good base to study the state of the art but they have not included the formation of intermetallic compounds within the assemblies. Limaye, et al.[13] studied the influence of intermetallics on Pb-free flip-chip solder joints using pure Sn as the Pb-free solder material. Their results showed that the inclusion of intermetallics in the models gave trends that have also been reported experimentally. They concluded that the inclusion of intermetallic layers presents some insight and explanation of joint behavior that previous assumptions of solder joint homogeneity cannot account for.

FEA on SAC Pb-free BGA's have so far not included intermetallic layers in the models. As shown by Limaye, et al. in their study using pure Sn, the inclusion of intermetallic layers in solder joint models gives results that can be correlated with

experimental results in a way that the homogeneous models studied by others have not. It is the focus of this study to include intermetallic layers in the geometries studied by FEM, an approach not taken in published literature found to date.

Conflicting results in reliability tests for backward compatible and Pb-free soldered assemblies has led to the practice of re-balling. This is mainly due to supply chain issues. The RoHS directive has filled the worldwide supply chain with components with Pb-free solder. Re-balling is the name given to the process of removing these Pb-free solder balls from the copper (Cu) pads of the BGA components received through the supply chain and replacing them with SnPb solder balls for re-assembly. A study soon to be published on the subject of re-balling has been recently conducted.[14] In this study the SAC solder balls were removed using solder wicks, the same procedure used on the manufacturing floors of aerospace industries. Table 2-3 summarizes the results of the study on the subject of re-balling.

Table 2-3 Results of Re-Balling Study

Study	Results
Study A	Solder mask defects (cracks exposing Cu) SAC bumps on Cu pads

As seen in Table 2-3, the results that stand out are:

1. the solder mask cracks exposing Cu

2. the removed Pb-free solder ball leaves behind some remnants of the Pb-free alloy on the Cu pads

As this study is unpublished to date, experiments taking these results into account have not been found in the literature. In much the same way, finite element modeling considering the effects of these Pb-free remnants on Cu pads after re-balling have not been found in the literature either. These Pb-free remnants give rise to new possible intermetallics that have not been taken into account in any experiment or FEA found to date. Comparison of the subsequent results of ATC tests in this case with experimental data has therefore not been found in the literature either. It is the focus of this study to include intermetallic layers in the geometries studied by FEM, an approach not taken in published literature found to date.

3 THEORETICAL REVIEW

3.1 ELECTRONIC PACKAGING

The word ‘packaging’ is commonly understood by the general engineering community as a container to prevent damage of a product during shipment. In the electronics industry the term ‘packaging’ refers to the placement and subsequent connection of electronic components in a protective enclosure that provides both security and access for system maintenance.[15] Figure 3-1 illustrates some important components involved in electronic packaging.

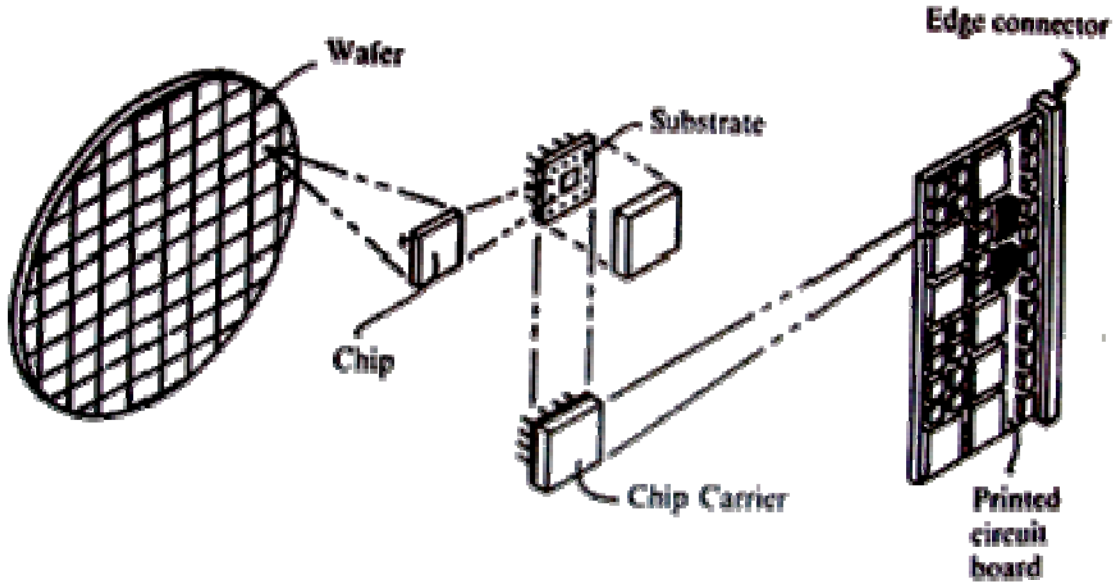

Figure 3-1 Components Involved in an Electronic Package[16]

In the packaging process wafers of silicon are fabricated using photolithographic semiconductor processes. Chips are diced from the wafers and integrated circuits made up of interconnected electronic devices, such as transistors and resistors, and are contained in these chips. Chip carriers are used to house these chips. Small wires or solder balls are used to electrically connect the chip and its carrier. These solder balls have traditionally been SnPb alloys. The chip carrier is often referred to as the first level of packaging and first level interconnection is the name attributed to electrical connections to the chip carrier. The bumps on the underside of the BGA package are used to connect the chip carrier to the PCB substrate.[16]

Second level packaging corresponds to the process of placing chip carriers on a circuit board or substrate and connecting them together with wiring traces, the second

level of interconnection. Then the edge connectors on the circuit boards being inserted into the back panel through contacts, allowing several circuit boards to communicate with each other, the third level of packaging and interconnection.

There are four major functions in the performance of electric and electronic systems that are served by electronic packaging. These functions are the drivers that advance the technology within the packaging industry. They include dissipation of generated heat, distribution of electrical power, interconnection of electrical signals and protection from the environment.

3.2 THERMOMECHANICAL MODELING OF SOLDER JOINTS – FINITE ELEMENT ANALYSIS

3.2.1 MODELS

Thermomechanical modeling of solder joints serves different purposes to different research teams. Some use resulting data from materials tests to formulate models that describe the constitutive behavior of solder materials or the evolution of damage. Others define and run tests used to make life predictions by either cycling joints until failure occurs or developing accelerated test methods that reduce test time yet capture failure mechanisms observed in experiments and actual service. In general, thermomechanical

modeling reduces a physical problem to a mathematical problem which can be solved to quantify pertinent parameters such as stress, strain, and energy density. The mathematical problems include (a) idealizations of solder joint geometries, (b) initial and boundary conditions, and (c) constitutive relations describing the behavior of the materials under study. The appropriate method for obtaining the solutions of these mathematical problems is the finite element method.

Solder joint geometries may be modeled in two dimensions (2-D) or three dimensions (3-D), an option mostly dependent on computing capacity. 3-D modeling works best in describing complex geometries yet many researchers model in 2-D allowing for simpler geometries and faster solutions that provide them with the desired results. Regardless of complexity the models address stresses, strains, deformations and damages in solder joints.

Initial conditions and boundary conditions must be established for proper thermomechanical modeling. The establishment of the initial conditions usually consists of specifying initial temperature at the start of an analysis, the initial stress of the joint or the initial microstructure of the joint. The boundary conditions describe the applied loads and are usually set by specifying the range of cycling temperatures, the ramp times between the temperature extremes and the hold times at specific temperatures.

The mathematical representation of the solder material response to the determined time-varying stimuli is enclosed in a constitutive model. Constitutive models abound and

one should not expect a single constitutive model to be perfect, or all-encompassing. A good model is defined as that which serves the particular purpose of the situation under study and serves the researcher as a tool to achieve the desired goal[10]. In the case of solder joints several constitutive models have been proposed, reviewed, modified and tested. An example is the set of constitutive models proposed by Darveaux which are used in the simulation of solder joint crack growth and fatigue life prediction. These models have been used by other researchers and results have confirmed the models as a good option for modeling the viscoplastic behavior of solder joints.[11 17] This has prompted several researchers, including several referred to in section 2 of this work, to adopt these models for their studies.

The finite element method allows the numerical modeling of solder joints for the study of multiple potential designs before experimental testing is used to verify the best one or two candidate designs. It is the method used in this study to evaluate backward compatible assemblies and re-balled assemblies to be used in aerospace products. Section 4 of this work describes the parameters used in this study in detail.

3.2.2 ANALYSIS METHODOLOGY

Results of inelastic energy density for the modeled geometries are obtained by analyzing the output generated by the commercial FEM package used, ANSYS 11.0. As seen in Figure 3-2 and Figure 3-4, the lower right quadrant of the solder ball geometry is divided into 100 evenly distributed spaces, making up a defined region for further

consideration of 100%. The lower right quadrant is chosen in these cases because the maximum energy density is located in that region. Figure 3-3 and Figure 3-5 highlight the lower right quadrants of the improperly mixed and properly mixed backward compatible assemblies, respectively. It should be noted that the re-balled assemblies follow the same procedure. The 10% of this region directly surrounding the point with the maximum energy density is the new area of interest, as defined in green in Figures3-2 to 3-5. The energy density in each of the evenly distributed spaces within this 10% region is added and subsequently multiplied by 10%, yielding the resulting energy density of the particular solder ball after ATC.

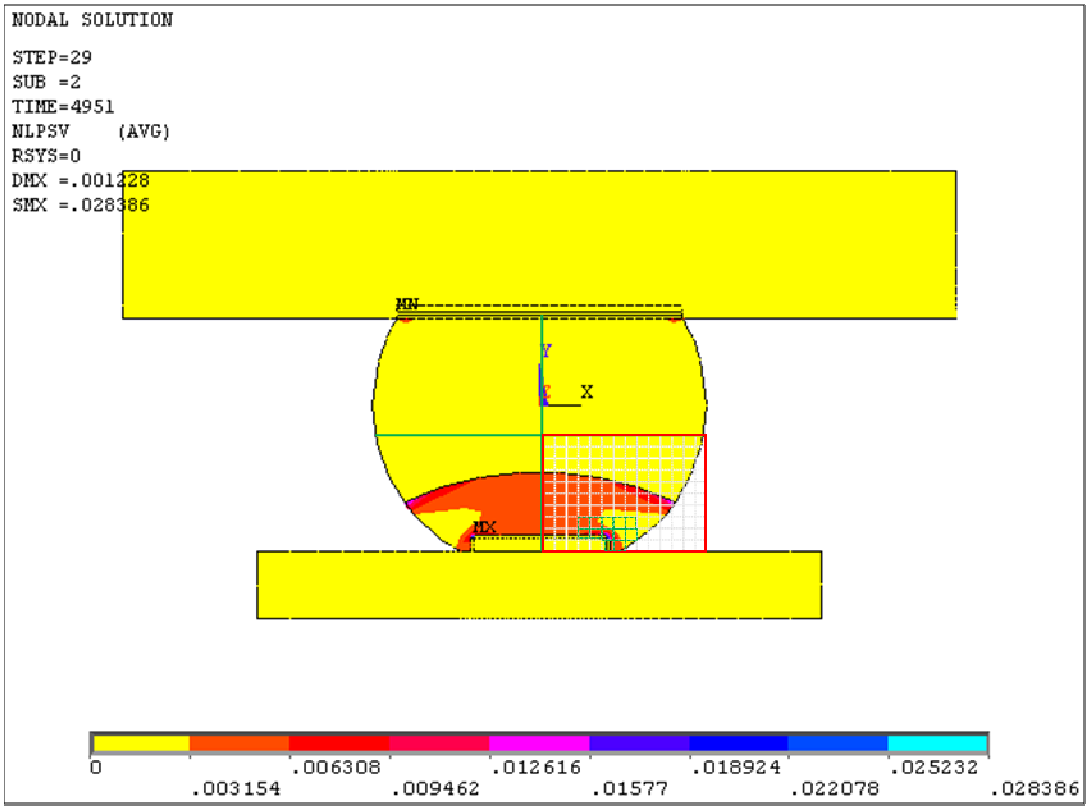

Figure 3-2 Improperly Mixed Backward Compatible Assembly Analysis Methodology

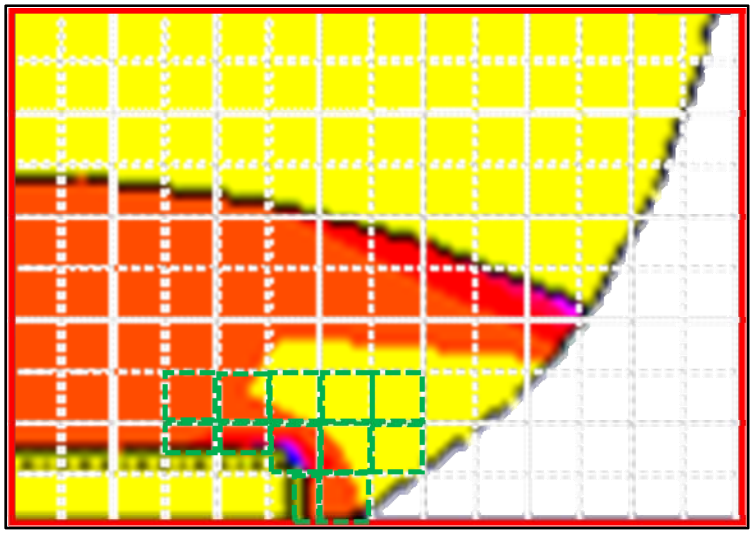

Figure 3-3 Highlight of Improperly Mixed Backward Compatible Assembly Analysis Methodology Showing 10% of Interest

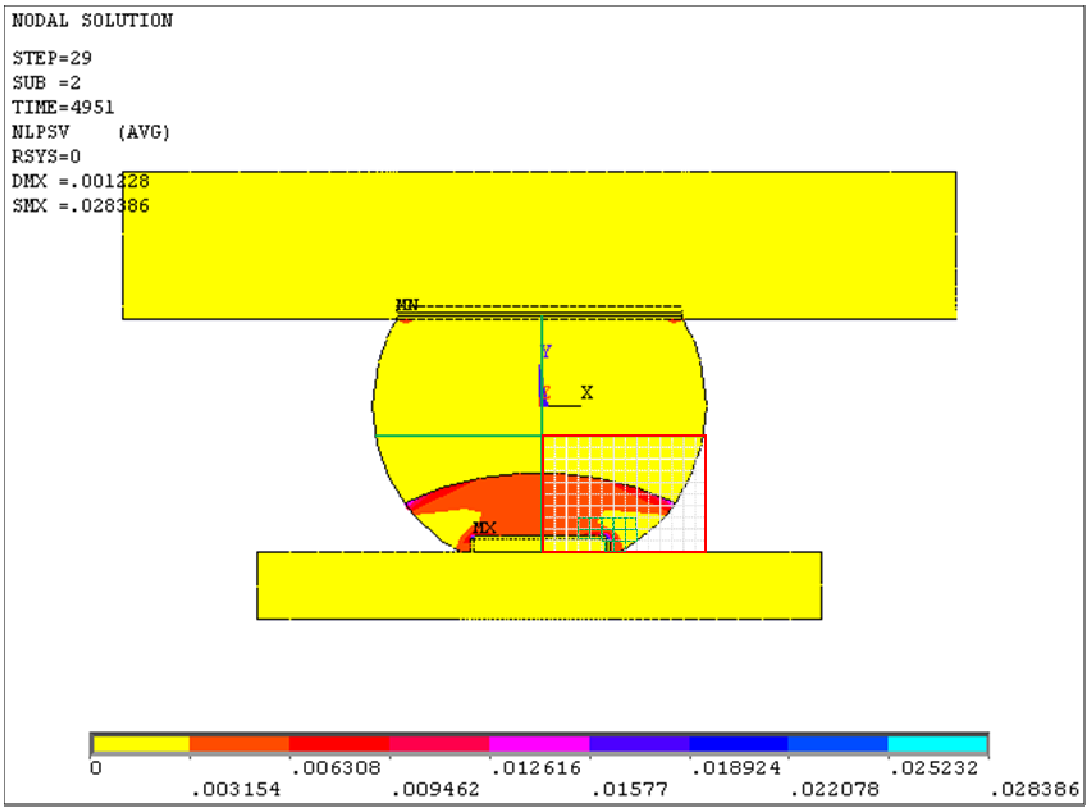

Figure 3-4 Properly Mixed Backward Compatible Assembly Analysis Methodology

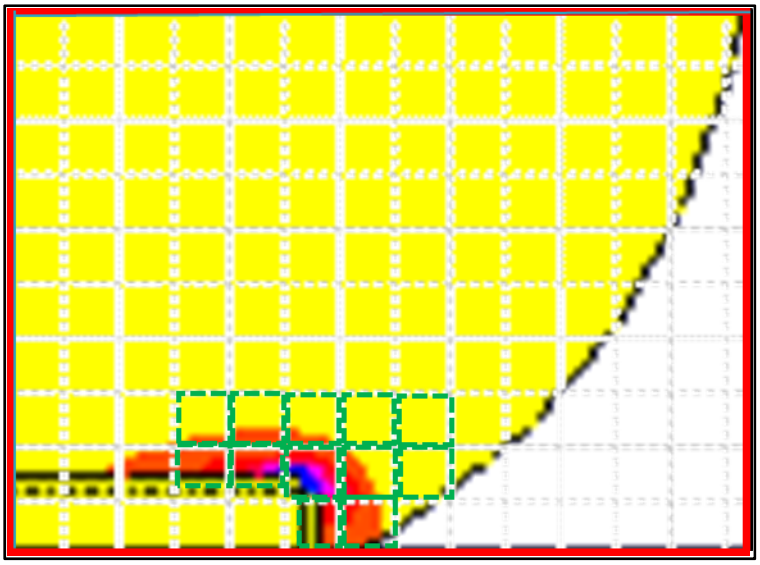

Figure 3-5 Highlight of Properly Mixed Backward Compatible Assembly Analysis Methodology Showing 10% of Interest

4 BALL GRID ARRAY CONFIGURATIONS

4.1 APPROACH

Reliability of solders in electrical components used for manufacturing of aerospace products is of utmost importance. Two accepted approaches used to study reliability are experiments and finite element analysis. The focus of this work is the BGA, a configuration typically used in electrical components of the aerospace industry. To this effect, experimental studies and finite element analysis used as reference pertain to that specific configuration of solder. In addition, these reference works have been conducted in the temperature range of interest, the temperature range typical of aerospace applications, as explained further on in this document.

Experimental tests have been carried out with BGAs consisting of Pb-free solder, specifically SAC alloys.[7] [8] They have also allowed researchers to see firsthand the formation of intermetallics due to the interaction of various metals. FEA of SAC solder

under the same conditions as the experimental studies has been previously carried out. Yet, the effect of intermetallic growth within solder balls has not been considered in these previous FEA. This study concentrates on FEA of SAC solder balls in a BGA, and the approach taken considers the effects of the intermetallic growth aforementioned. The intention of this consideration is to model the solder ball under study with the expected intermetallic growth in order to observe the effect of ATC on SAC solder more specifically and its subsequent effect on reliability. Figure 4-1 depicts the general approach taken in this study[12]. Let us proceed to discuss the steps taken in the approach in more detail.

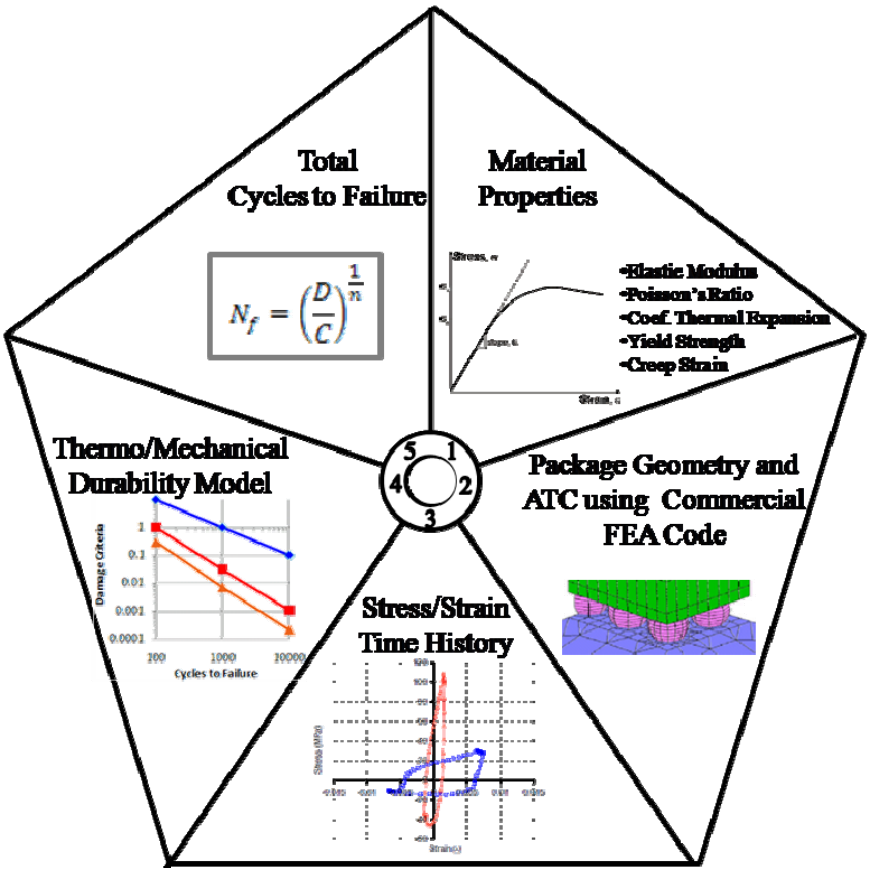

Figure 4-1 General Approach

The first step was to define the constitutive properties of the materials under study. These material properties serve as inputs in the FEM in order to take into account the viscoplastic behavior of the materials. The properties of the solders, the intermetallics and other components of the electronic package can be seen in sections 4.2 and 4.3. Commercial FEA code was then used to build the various geometries studied. The modeled geometries are discussed in more detail in section 4.4. This package, ANSYS 11.0, was then used to simulate thermal cycling tests. The thermal cycles to which they were subjected can be seen in section 4.5. Potential failure site within the solder ball can then be identified using the finite element tests. This is based on maximum accumulated damage in the solder ball which can be observed through creep strain and energy density results, outputs of the process. These processes correspond to steps 1-3 in Figure 4-1.

Implementation of the above approach to BGA assemblies of backward compatible Pb-free solders and re-balled SnPb solders is now presented in the next sections. Two-dimensional FEM and stress analysis of two thermal cycling tests for both Sn37Pb and Sn3.8Ag0.7Cu solders are presented. Results are then compared and analyzed.

4.2 MATERIAL MODEL FOR SAC AND SNPB

There is a wide variety of Pb-free solders under study in the scientific community, and within this variety there are many different SAC alloys. The lack of standardization

of SAC has led to inconsistencies in the published mechanical properties of this family of Pb-free alloys. These inconsistencies are mainly due to the differences in preparation procedures, varying concentrations of Ag and Cu and varying data collection procedures. Thus the constitutive models for eutectic SnPb and Sn3.8Ag0.7Cu used in this FEA study were established as described below.[11]

4.2.1 MODULUS OF ELASTICITY

The modulus of elasticity of each of the materials is a function of temperature, giving rise to the need of constitutive models. Darveaux, et al. performed a comparative study of various models for the determination of the modulus of elasticity for SnPb and SAC. [18] Results showed that differences between experimental results and the model resulting from the equations below were of approximately 5%. Thus the equations proposed by Darveaux, et al. for the modulus of elasticity constitutive model for both SnPb and SAC have been chosen for this study, as can be seen in Equation 4-1 and Equation 4-2. In both cases, temperatures are in °C and the resulting modulus of elasticity is in MPa. Figure 4-2 shows results of the model for temperatures of interest.

SnPb:

$$E = 35366 - 151T$$ **Equation 4-1**

SAC:

$$E = 52400 - 193.05T$$ **Equation 4-2**

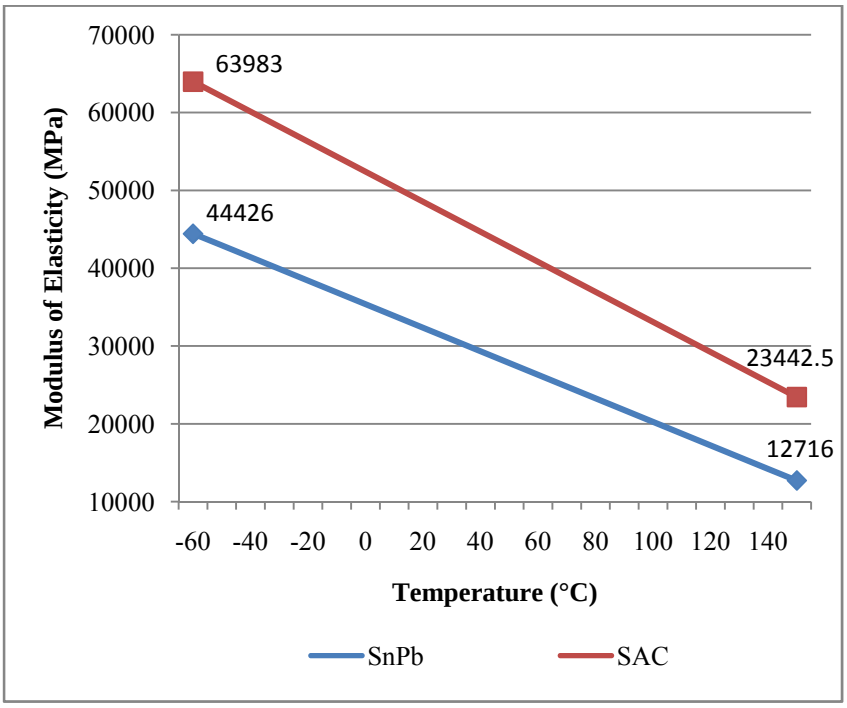

Figure 4-2 Results for Modulus of Elasticity Constitutive Models for SnPb and SAC

4.2.2 YIELD STRENGTH

Good data for the yield strength of SAC, specifically Sn3.8Ag0.7Cu, is not readily available in literature. This is mostly due to the lack of standardization

aforementioned. The use of plasticity data for Sn seems to be an option at first glance, yet close attention should be paid to the implications of using data corresponding to that single alloying element. The effects of the Ag and Cu are clearly seen in the final properties of SAC when considering that data corresponding to yield strength and modulus of elasticity of Sn do not correspond to the observed behavior of SAC. Therefore, Plastic behavior will be neglected and creep will be the only inelastic behavior considered.

4.2.3 CREEP STRAIN

Several constitutive models for creep strain have been published. This study will follow the model discussed by Weise, et al. [19], a model which is based on experimental tests done on solder joints of real size and has been adopted by other research teams including Vandevelde, et al.[11]. The equations used for the constitutive model of the creep strain of the materials under study are presented below. In both equations used, temperatures are in K and σ is in MPa. Tables 4-1 and 4-2 show the coefficients of the models for temperatures of interest.

SnPb:

$$\dot{\varepsilon}_{cr} = c_1[\sinh(c_2\sigma)]^{c_3} e^{-c_4/T} \qquad \textbf{Equation 4-3}$$

where

$\dot{\varepsilon}_{cr}$ = change in equivalent creep strain with respect to time

σ = equivalent stress

T = temperature in K.

SAC:

$$\dot{\varepsilon}_{cr} = c_1 \sigma^{c_2} e^{-c_3/T}$$ **Equation 4-4**

where

$\dot{\varepsilon}_{cr}$ = change in equivalent creep strain with respect to time

σ = equivalent stress

T = temperature in K

Table 4-1 Coefficients for SnPb Creep Strain Constitutive Model[11]

Temperature (K)	C1	C2	C3	C4
213	1280.8	0.0456	3.3	6352
423	184.58	0.159	3.3	6352

Table 4-2 Coefficients for SAC Creep Strain Constitutive Model[11]

Temperature (K)	C1	C2	C3
298	2e-21	18	9994.59

4.2.4 COEFFICIENT OF THERMAL EXPANSION (CTE) AND POISSON'S RATIO

The coefficient of thermal expansion of SAC and SnPb are found in literature, as well as the respective Poisson's Ratios.[11] Table 4-3 lists these values.

Table 4-3 Coefficient of Thermal Expansion and Poisson's Ratio for SAC and SnPb Solders[11]

Material	CTE	Poisson's Ratio
SAC	17.6 x10^{-6}/°C	0.33
SnPb	25.5 x10^{-6}/°C	0.4

4.2.5 PWB, TERMINATION AND COMPONENTS

The values for the elastic modulus, Poisson's ratio and coefficient of thermal expansion of the PWB and the Cu were also considered in the model and are listed in Table 4-4.

Table 4-4 Material Properties for PWB, Termination and Components[1120]

Temperature (298K)	Elastic Modulus (MPa)	Poisson's Ratio	CTE
FR-4 PWB	25,700	0.4	20 x10^{-6}/°C
Cu	117,000	0.35	16 x10^{-6}/°C

4.3 INTERMETALLIC PROPERTIES

The formation of intermetallics has been considered in the FEM. Published literature on Sn-based intermetallics indicates that these intermetallics tend to be brittle in nature.[13] This means that so long as the yield stress limit was not exceeded, an elastic behavior assumption was valid. The location of any failure was in the solder joint, not at the interfaces. This points to ductile fracture. Intermetallic growth due to aging was not considered. Also, the layer of intermetallics was modeled as continuous and any spalling of this layer was not considered. Any microstructural evolution of the solder joint was also neglected. The particular material properties of these intermetallics and the locations in which they form can be seen in greater detail in the discussion of the modeled geometries in section 4.4.

4.4 MODELS AND GEOMETRIES

Backward compatible and re-balled assemblies were modeled in this study in order to achieve the set objectives. The details of each are presented below.

4.4.1 BACKWARD COMPATIBLE ASSEMBLIES

The backward compatible assembly modeled consists of a SAC solder ball and SnPb solder paste. Three different size soldered balls were modeled, their respective sizes being 0.5mm diameter and 0.2mm height, 0.75mm diameter and 0.3mm height, and 1.0mm diameter and 0.4mm height. Two different scenarios were modeled for each of these three geometries, a properly mixed assembly and an improperly mixed assembly. In the properly mixed scenarios the bulk of the solder ball is modeled as SAC and intermetallic formation is modeled at the interface with the Cu pads. In the improperly mixed scenarios the bulk of the solder is divided into two sections: one third of the bulk is modeled as a SAC/SnPb mixture and the remaining two thirds of the bulk are modeled as SAC. Again, additional intermetallic formation at the interface with the Cu pads is modeled. Each of these three solder geometries in each of the two scenarios described were subjected to ATC in the FEM. The ATC specifics are described in section 4.5. Table 4-5 and Table 4-6 present detail of the distribution of the intermetallics in the modeled geometries.[21] [22] Figures 4-3 and 4-4 present diagrams of these distributions.

Table 4-5 Distribution of Materials in Properly Mixed Backward Compatible Geometries

Depth from top	SAC Elastic Modulus (GPa)
0-10 μm	86.4 (Intermetallic 1 – SAC/Cu)
10-18 μm	50.0 (Intermetallic 2 – SAC/Cu)
Bulk @room temperature	48.0
Last 10 μm	84.310 (Intermetallic 3 - SAC/SnPb/Cu)

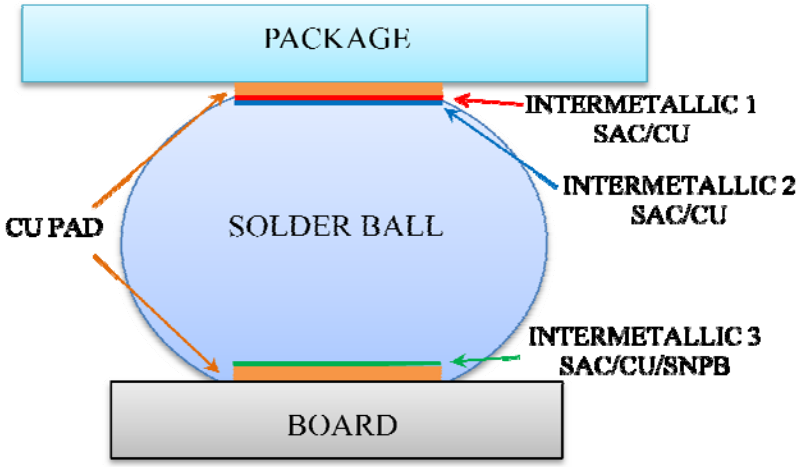

Figure 4-3 Diagram of Distribution of Materials in Properly Mixed Backward Compatible Geometries

Table 4-6 Distribution of Materials in Improperly Mixed Backward Compatible Geometries

Depth from top	SAC Elastic Modulus (GPa)
0-10 µm	86.4 (Intermetallic 1 – SAC/Cu)
10-18 µm	50.0 (Intermetallic 2 – SAC/Cu)
2/3 Bulk @room temperature	48.0 *
1/3 Bulk @room temperature	42.32 (SAC/SnPb) *
Last 10 µm	84.310 (Intermetallic 3 - SAC/SnPb/Cu)

*An abrupt property change was modeled to simulate improper SnPb/SAC mixing.

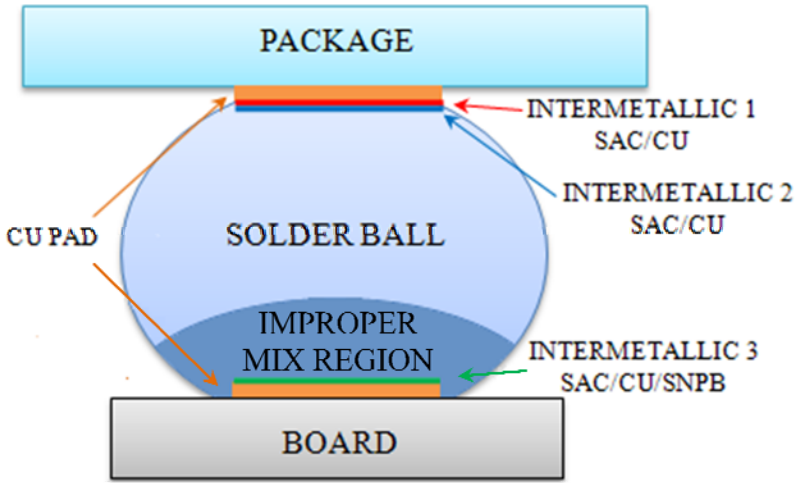

Figure 4-4 Diagram of Distribution of Materials in Improperly Mixed Backward Compatible Geometries

4.4.2 RE-BALLED ASSEMBLIES

Re-balling is the term assigned to the process of removing SAC solder balls from SnPb paste and placing SnPb solder balls in their place. Experiments have been carried out in order to see the results of the re-balling process when the SAC solder balls are removed with solder wicks, a procedure that mimics the reality of aerospace industry manufacturing floors.[11] Results show that the ball removal process leaves traces of SAC solder on the SnPb paste and that these traces are not removed. Thus, when a new SnPb solder ball is placed on the SnPb paste where the SAC solder ball used to be, the traces of SAC are left between this new SnPb solder ball and the SnPb paste. The final re-balled assembly therefore consists of a SnPb solder ball, a thin layer of trace SAC, and SnPb paste. In the re-balled assembly modeled the SnPb solder ball is directly over a thin layer

of SAC/Cu intermetallic, which is itself over the SnPb paste. This thin layer of the SAC/Cu intermetallic modeled serves the purpose of including the effects of re-balling found in experimental studies. Three different size soldered balls were modeled, their respective sizes being 0.5mm diameter and 0.2mm height, 0.75mm diameter and 0.3mm height, and 1.0mm diameter and 0.4mm height. Each of these three solder geometries were subjected to ATC in the FEM. The ATC specifics are described in section 4.5. The bulk of the solder ball was modeled as SnPb and the detailed intermetallic distribution is presented in Table 4-7. Figure 4-5 presents a diagram of this distribution.

Table 4-7 Distribution of Materials in Re-Balled Geometries

Depth from top	SnPb Elastic Modulus (GPa)
0-10 μm	86.4 (Intermetallic 1 – SAC/Cu) **
10-18 μm	31.591
Bulk @room temperature	31.591
Last 10 μm	84.310 (Intermetallic 2 - SAC/SnPb/Cu)

**This intermetallic layer was left in the re-balled model to simulate SAC solder residuals from the re-balling process.

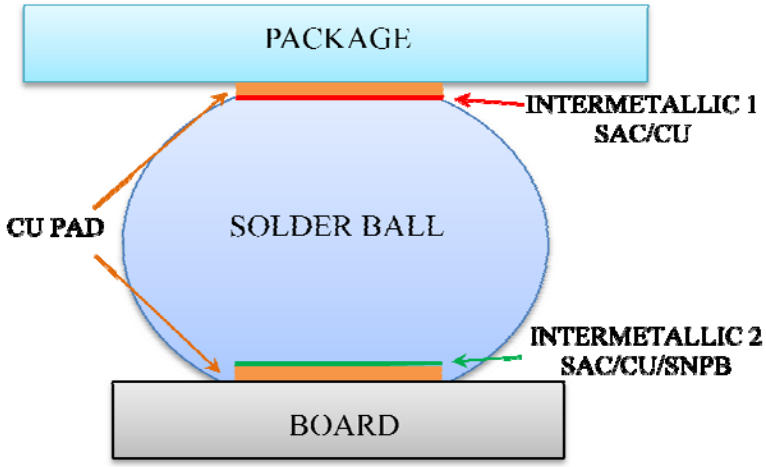

Figure 4-5 Diagram of Distribution of Materials in Re-Balled Geometries

4.5 ACCELERATED THERMAL CYCLING LOADING CONDITIONS

Each of the geometries described in section 4.4 were subjected to ATC through the FEA package. The two accelerated loading conditions applied to each of the geometries are listed in Table 4-8, along with the specifics of cycle time, ramp-up time and dwell time. These thermal loads correspond to the experimental loads of the studies by Nandagopal, et al. and Bath, et.al., allowing the comparison of the FEA results of this work with their experimental results.

Table 4-8 Thermal Loading Conditions for FEA

ID	Range (°C)	Cycle Time (min)	Ramp-Up Time (min)	Dwell Time (min)
1	0 to 100	30	5	10
2	-40 to 125	60	15	15

5 RESULTS AND ANALYSIS

5.1 SNPB ASSEMBLY AND PB-FREE ASSEMBLY

A 0.5mm solder ball SnPb assembly and a 0.5mm solder ball SAC assembly were modeled as a baseline, much like Bath et al., Nandagopal et al. and suggested by Vandevelde, et al. in their FEA study. These geometries were subjected to cycle 1 and cycle 2. Results were compared to those presented in sections 5.2 and 5.3 corresponding to backward compatible assemblies. As can be seen in the following figures, FEA damage results taking energy density as the analysis method are consistent with experimental findings, showing that this analysis approach is better that the inelastic strain per cycle averaged over damage volume. These results correlate with those of Limaye, et al. Thus, the results presented in the following sections for backward compatible assemblies and re-balled assemblies correspond to this method, energy density.

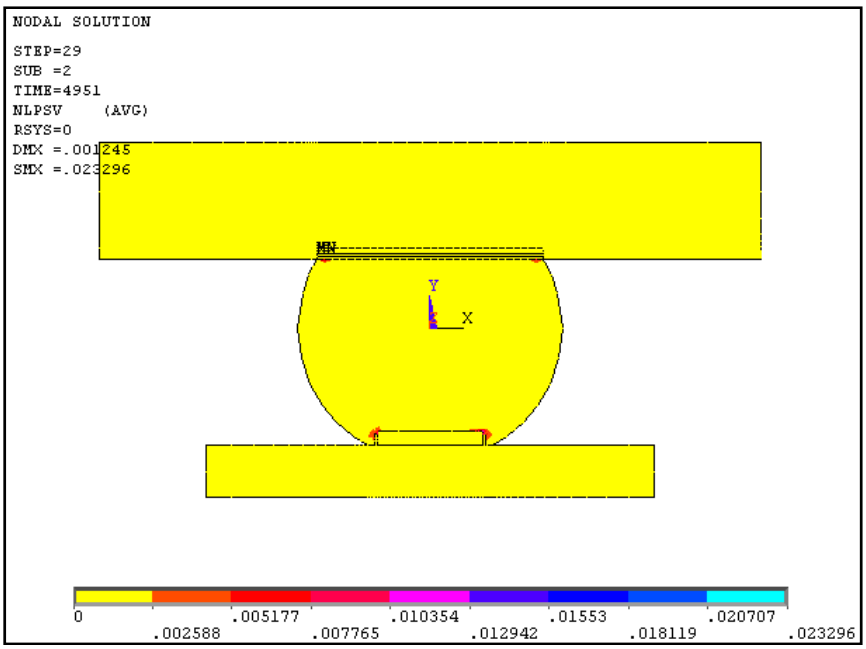

Figure 5-1 SnAgCu Assembly Inelastic Energy Density Results, Cycle 1

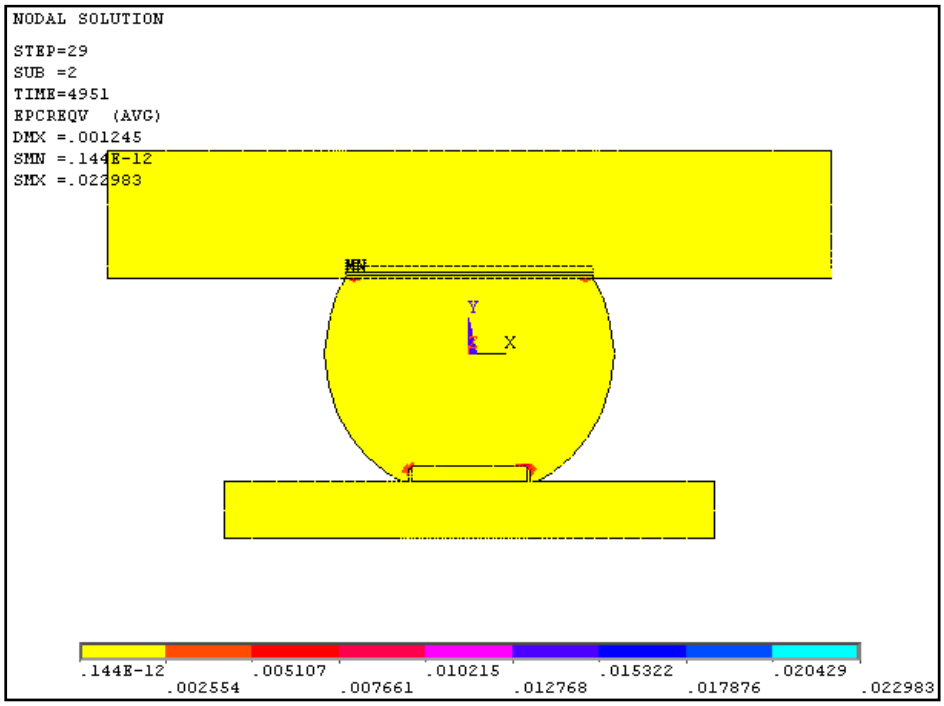

Figure 5-2 SnAgCu Assembly Inelastic Strain, Cycle 1

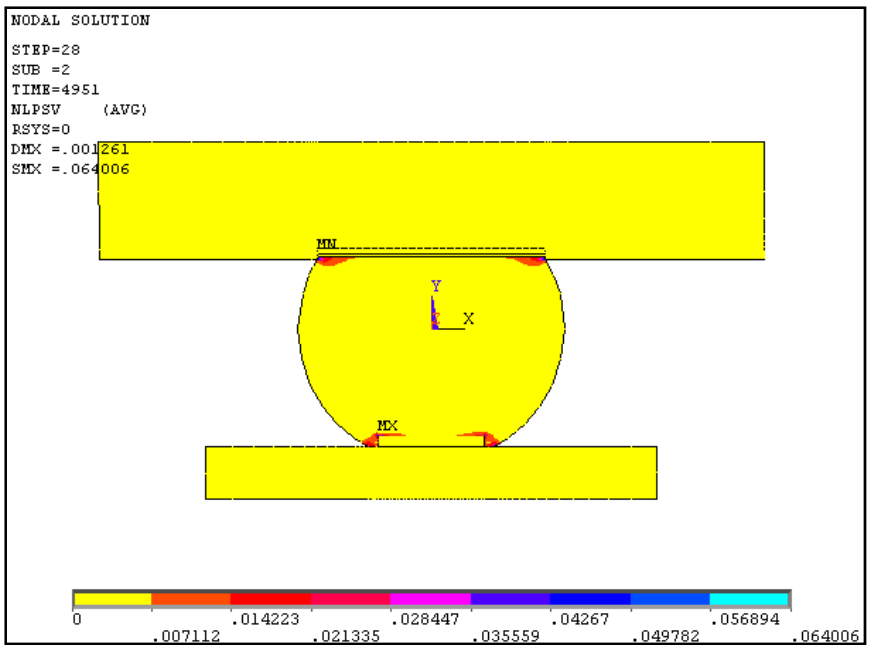

Figure 5-3 SnPb Assembly Inelastic Energy Density Results, Cycle 1

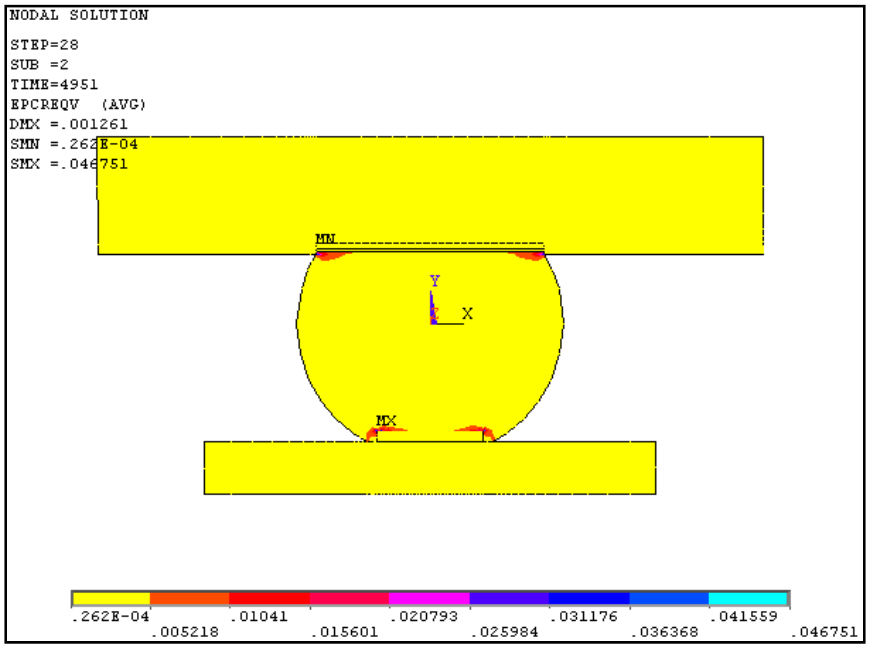

Figure 5-4 SnPb Assembly Inelastic Strain, Cycle 1

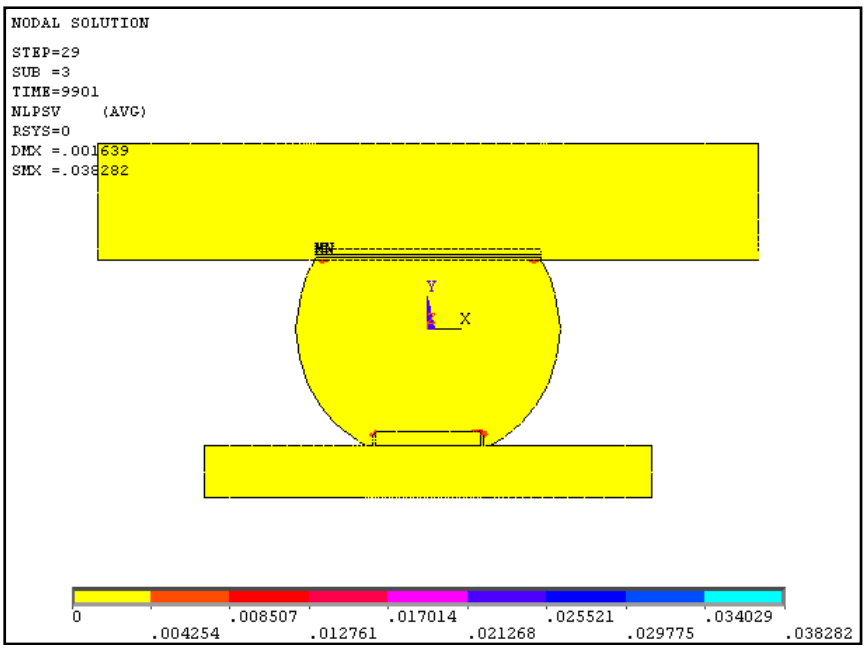

Figure 5-5 SnAgCu Assembly Inelastic Energy Density Results, Cycle 2

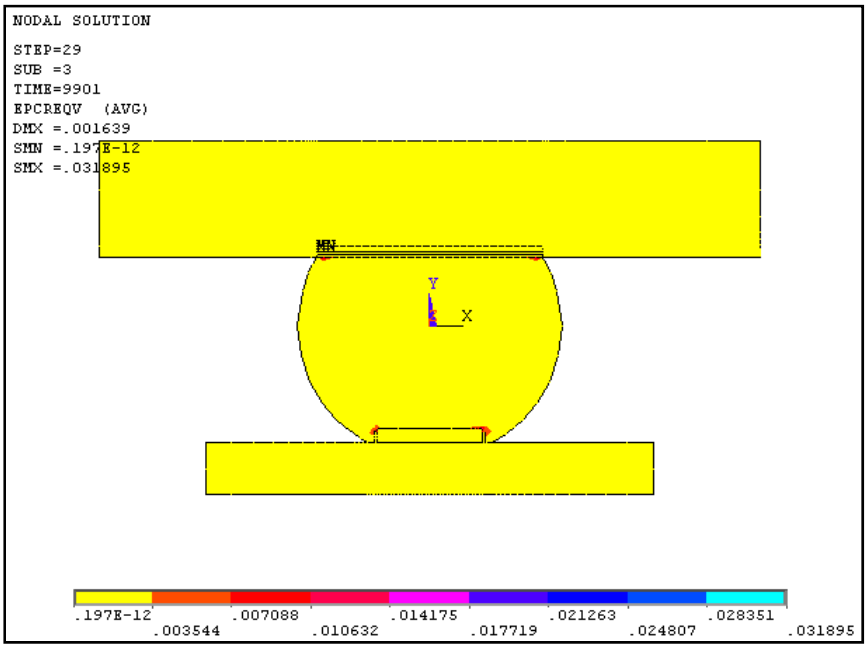

Figure 5-6 SnAgCu Assembly Inelastic Strain, Cycle 2

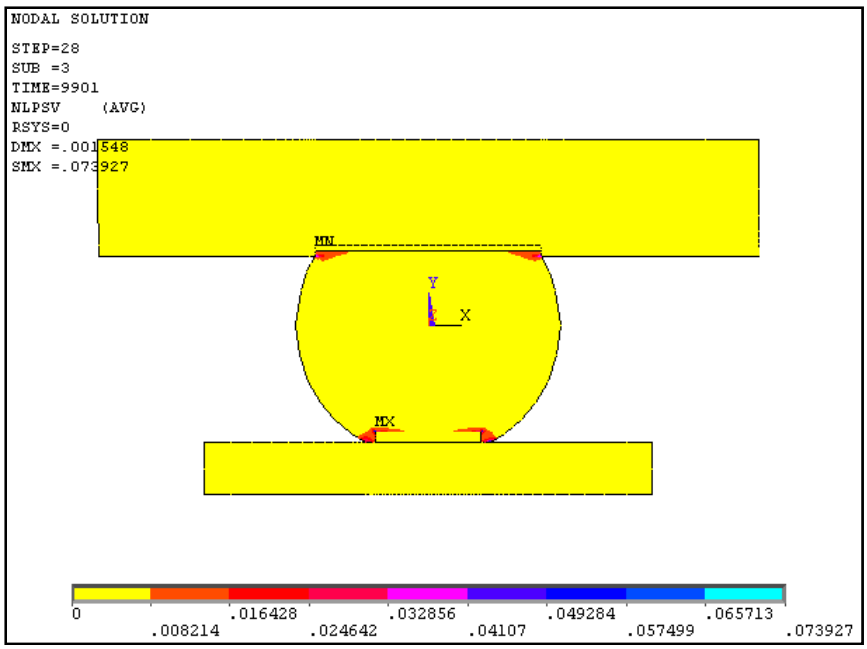

Figure 5-7 SnPb Assembly Inelastic Energy Density Results, Cycle 2

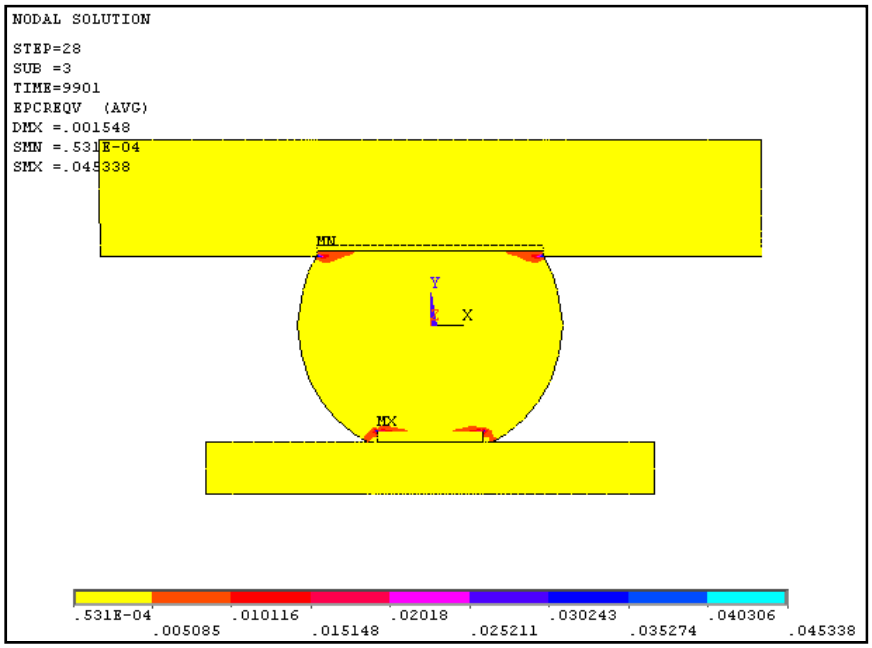

Figure 5-8 SnPb Assembly Inelastic Strain, Cycle 2

5.2 BACKWARD COMPATIBLE ASSEMBLY

Section 5.2 presents results for improperly mixed solder balls and section 5.3 presents results for properly mixed solder balls.

5.2.1 IMPROPERLY MIXED BY DIAMETER

5.2.1.1 0.5MM BALLS – CYCLE 1 VS CYCLE 2

The 0.5mm improperly mixed solder balls subjected to cycle 1 and cycle 2 showed a similar affected area, mostly within the region of the SAC/SnPb improper mixture. The energy density in the bulk of the mixture region is 0.003154MPa for cycle 1 and 0.004501MPa for cycle 2. Closer examination shows an increase in the energy density in the regions closest to the division between the materials for both balls, particularly toward their outer corners. This increase can also be seen close to the Cu pads of the assemblies, particularly in the square corners of the pads, and reaches values of 0.012616MPa for cycle 1 and 0.018003MPa for cycle 2. The maximum energy density for cycle 1 is 0.028386MPa and 0.04050MPa for cycle 2. Thus, the 0.5mm improperly mixed solder ball subjected to cycle 2 has higher energy density than the same solder ball subjected to cycle 1.

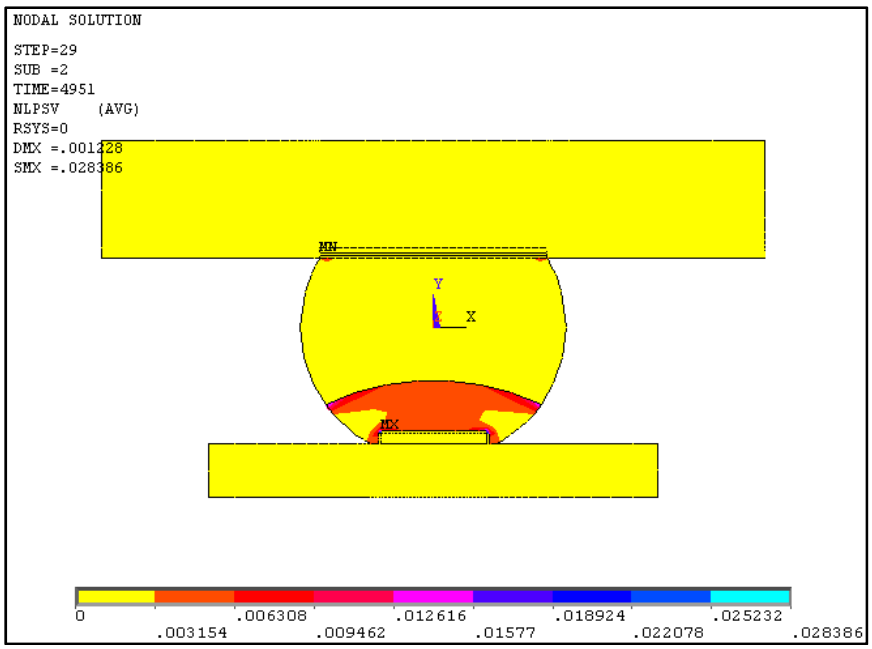

Figure 5-9 Backward compatible assembly, 0.5mm diameter, Cycle 1, improperly mixed solder ball

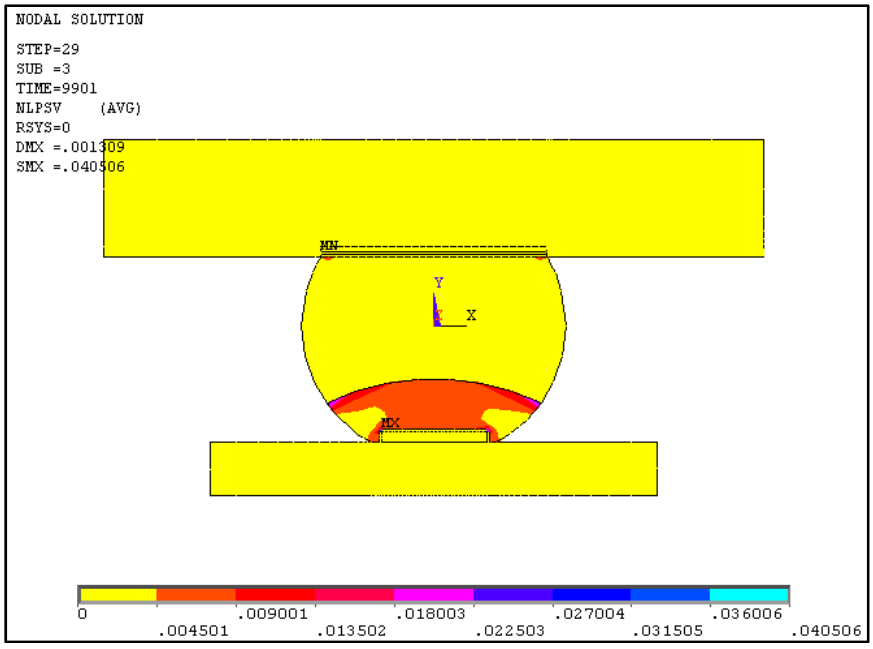

Figure 5-10 Backward compatible assembly, 0.5mm diameter, Cycle 2, improperly mixed solder ball

5.2.1.2 0.75MM BALLS – CYCLE 1 VS CYCLE 2

The 0.75mm improperly mixed solder balls subjected to cycle 1 and cycle 2 showed a similar affected area, mostly within the region of the SAC/SnPb improper mixture. As can be seen, the energy density in the region closest to the division between materials in the bulk of the mixture is 0.003744MPa for cycle 1 and 0.005188MPa for cycle 2. The energy density toward their outer corners of the balls and close to the Cu pads of the assemblies shows an increase, reaching values of 0.014975MPa for cycle 1 and 0.020753MPa for cycle 2. The maximum energy density for cycle 1 is 0.033694MPa and 0.046694MPa for cycle 2. Thus, the 0.75mm improperly mixed solder ball subjected to cycle 2 has higher energy density than the same solder ball subjected to cycle 1.

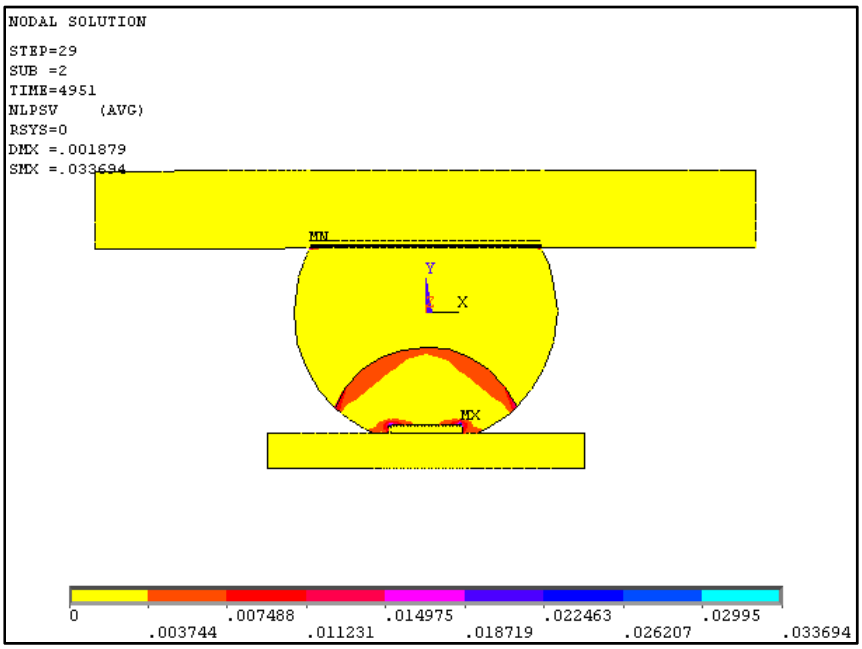

Figure 5-11 Backward compatible assembly, 0.75mm diameter, Cycle 1, improperly mixed solder ball

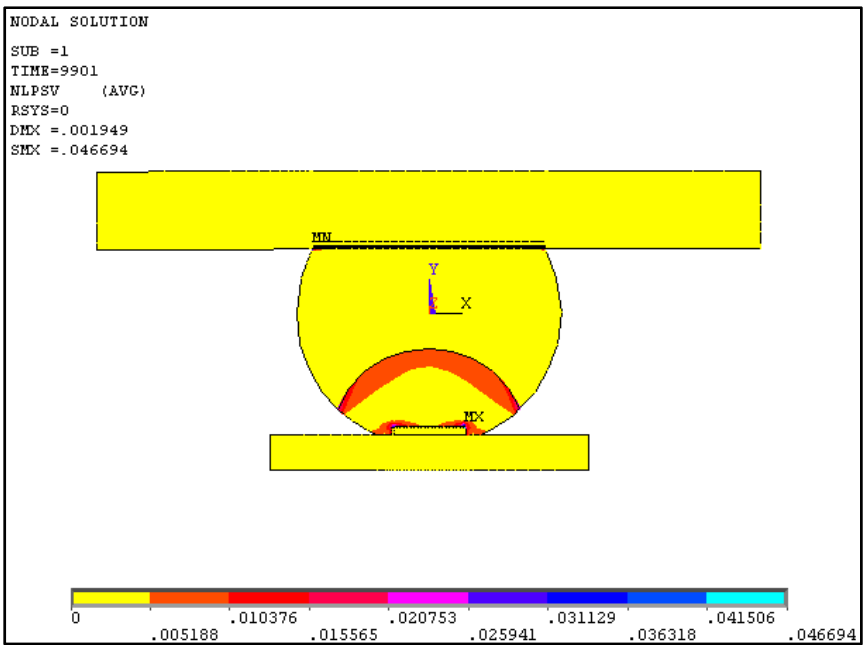

Figure 5-12 Backward compatible assembly, 0.75mm diameter, Cycle 2, improperly mixed solder ball

5.2.1.3 1.0MM BALLS – CYCLE 1 VS CYCLE 2

The 1.0mm improperly mixed solder balls subjected to cycle 1 and cycle 2 showed a similar affected area, mostly within the region of the SAC/SnPb improper mixture. The most noticeable energy density in the bulk of the solder balls is present in the areas outlining the divisions between the materials. This extends throughout the curves and continues to cover the areas directly around the Cu pads. The energy density in these regions is 0.003639MPa for cycle 1 and 0.005294MPa for cycle 2. The maximum values observed toward the outer corner of the solder balls and surrounding the Cu pads are 0.014556MPa for cycle 1 and 0.021177MPa for cycle 2. The maximum energy density values are 0.032752MPa for cycle 1 and 0.047649MPa for cycle 2. Thus,

the 1.0mm improperly mixed solder ball subjected to cycle 2 has higher energy density than the same solder ball subjected to cycle 1.

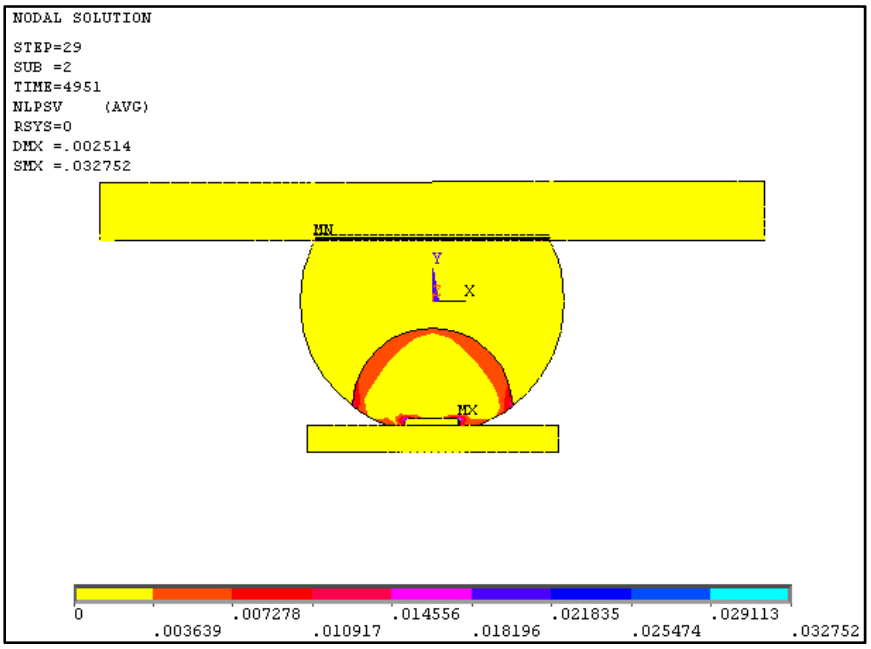

Figure 5-13 Backward compatible assembly, 1.0mm diameter, Cycle 1, improperly mixed solder ball

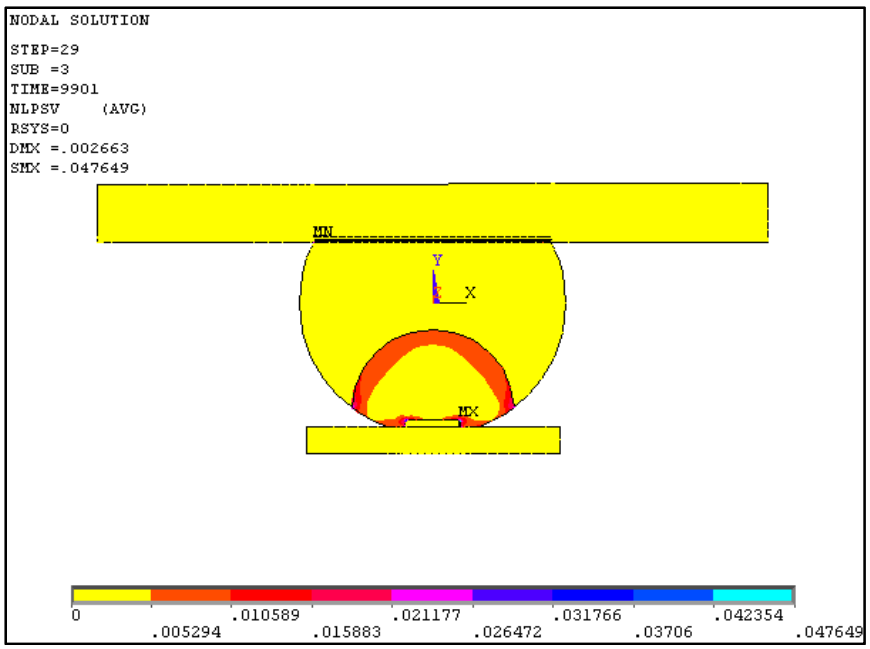

Figure 5-14 Backward compatible assembly, 1.0mm diameter, Cycle 2, improperly mixed solder ball

5.2.2 IMPROPERLY MIXED BY CYCLE

5.2.2.1 CYCLE 1 – 0.5MM VS 0.75MM VS 1.0MM BALLS

The three solder balls present variations in energy density throughout their bulk in comparison to each other. The 0.5mm solder ball has an affected area of roughly one third of the size of the bulk, with an energy density of 0.003154MPa. The 0.75mm and 1.0mm balls show affected areas of similar size in relation to the size of the bulk with the 1.0mm ball having a slightly smaller affected area. The 1.0mm ball shows a lower energy density of 0.003639MPa than the 0.75mm ball with an energy density of 0.003744MPa. Thus, results show that the energy density, and its maximum value,

increases from the 0.5mm ball to the 0.75mm ball but decreases from the 0.75mm ball to the 1.0mm ball. The actual area affected by this energy density is notably greater for the 0.5mm ball than for the other two, with about one third of the ball being affected. In all three cases the maximum values of energy density were concentrated along the division between the material regions and toward the outer corners of the balls, pointing to these locations as the most critical for reliability.

5.2.2.2 CYCLE 2 – 0.5MM VS 0.75MM VS 1.0MM BALLS

The three solder balls present variations in energy density throughout their bulk in comparison to each other. The 0.5mm solder ball has an affected area of roughly one third of the size of the bulk, with an energy density of 0.004501MPa. The 0.75mm and 1.0mm balls show affected areas of similar size in relation to the size of the bulk with the 1.0mm ball having a slightly smaller affected area. The 1.0mm ball shows a higher energy density of 0.005294MPa than the 0.75mm ball with an energy density of 0.005188MPa. Thus, results show that the energy density, and its maximum value, increases as the size of the solder ball increases. Yet, the actual area affected by this energy density decreases as the size of the solder ball increases, making the 0.5mm solder ball more affected than the 1.0mm solder ball despite the smaller numerical value of the energy density of the first over the latter. In all three cases the maximum values of energy density were concentrated along the division between the material regions and

toward the outer corners of the balls, pointing to these locations as the most critical for reliability.

5.2.2.3 IMPROPERLY MIXED GLOBAL RESULTS

Figure 5-15 shows a plot with the results for all three solder ball geometries under each of the two thermal cycles. The solder balls subjected to cycle 2 show an acceleration factor of 1.4 over the solder balls subjected to cycle 1 for all three geometries. The case with the highest energy density corresponds to the 1.0mm solder ball subjected to cycle 2 and the case with the lowest energy density corresponds to the 0.5mm solder ball subjected to cycle 1.

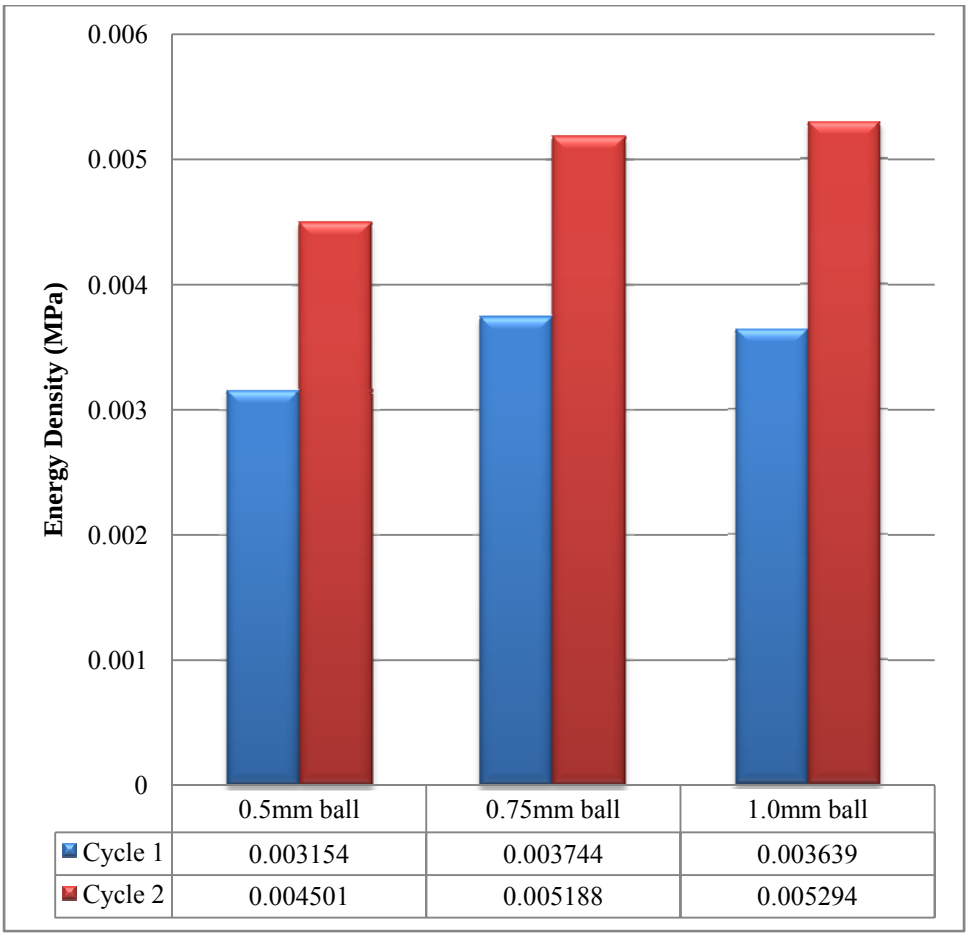

Figure 5-15 Energy Density Results for Improperly Mixed Backward Compatible Assemblies

5.2.3 PROPERLY MIXED BY DIAMETER

5.2.3.1 0.5MM BALLS – CYCLE 1 VS CYCLE 2

The 0.5mm properly mixed solder balls subjected to cycle 1 and cycle 2 showed a similar affected area, mostly just at the upper and bottom corners of the balls. The energy

density in the case of cycle 1 is 0.003591MPa. In the case of cycle 2 the corresponding value is 0.005156MPa. The maximum energy density for cycle 1 is 0.032318MPa and 0.046404MPa for cycle 2. Thus, the 0.5mm properly mixed solder ball subjected to cycle 2 has higher energy density than the same solder ball subjected to cycle 1.

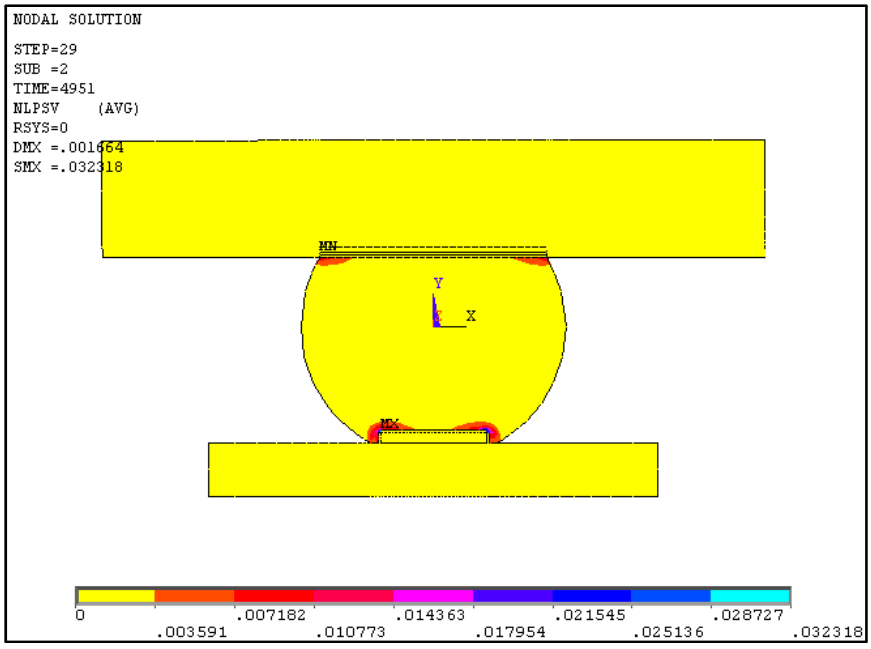

Figure 5-16 Backward compatible assembly, 0.5mm diameter, Cycle 1, properly mixed solder ball

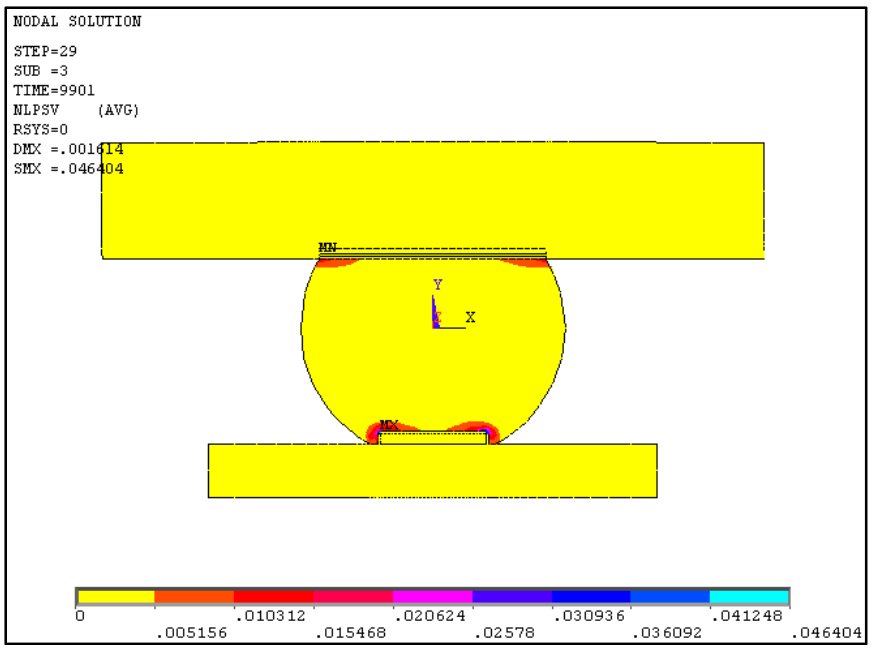

Figure 5-17 Backward compatible assembly, 0.5mm diameter, Cycle 2, properly mixed solder ball

5.2.3.2 0.75MM BALLS – CYCLE 1 VS CYCLE 2

The 0.75mm properly mixed solder balls subjected to cycle 1 and cycle 2 showed a similar affected area, mostly just at the upper and bottom corners of the balls. The energy density in the case of cycle 1 is 0.003695MPa. In the case of cycle 2 the corresponding value is 0.005223MPa. The maximum energy density for cycle 1 is 0.033251MPa and 0.047006MPa for cycle 2. Thus, the 0.75mm properly mixed solder ball subjected to cycle 2 has higher energy density than the same solder ball subjected to cycle 1.

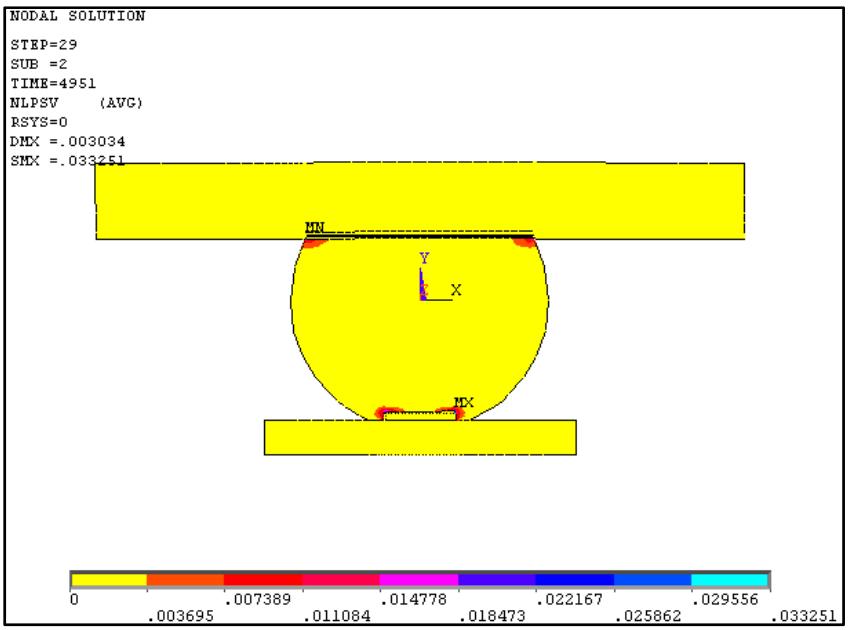

Figure 5-18 Backward compatible assembly, 0.75mm diameter, Cycle 1, properly mixed solder ball

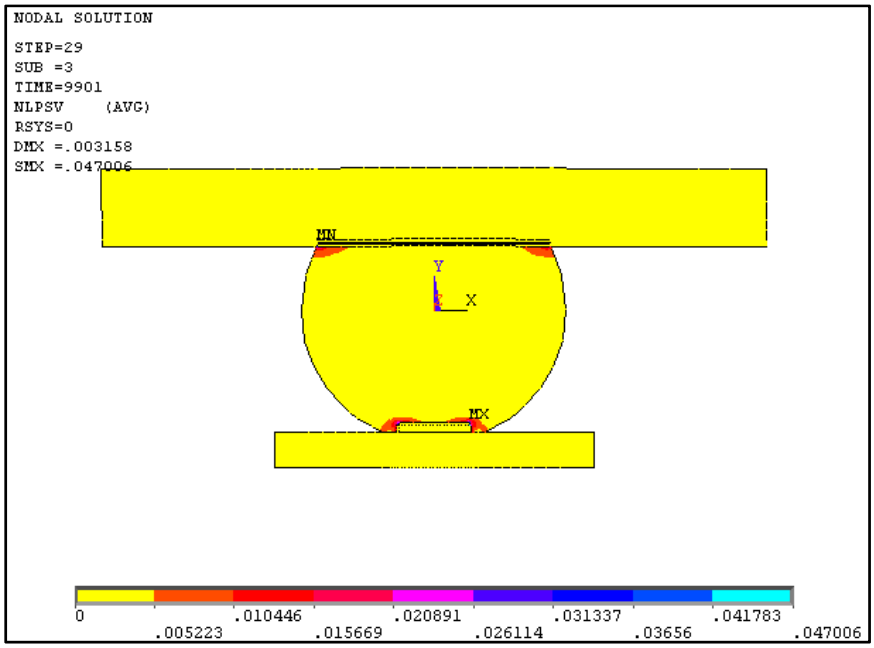

Figure 5-19 Backward compatible assembly, 0.75mm diameter, Cycle 2, properly mixed solder ball

5.2.3.3 1.0MM BALLS – CYCLE 1 VS CYCLE 2

The 1.0mm properly mixed solder balls subjected to cycle 1 and cycle 2 showed a similar affected area, mostly just at the upper and bottom corners of the balls. The energy density in the case of cycle 1 is 0.003446MPa. In the case of cycle 2 the corresponding value is 0.004953MPa. The maximum energy density for cycle 1 is 0.03101MPa and 0.044574MPa for cycle 2. Thus, the 1.0mm properly mixed solder ball subjected to cycle 2 has higher energy density than the same solder ball subjected to cycle 1.

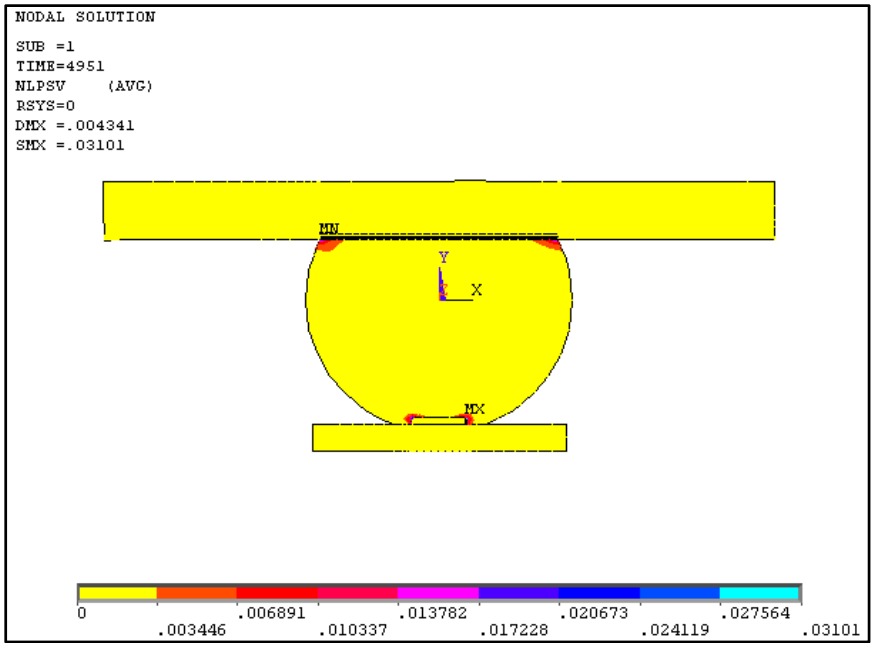

Figure 5-20 Backward compatible assembly, 1.0mm diameter, Cycle 1, properly mixed solder ball

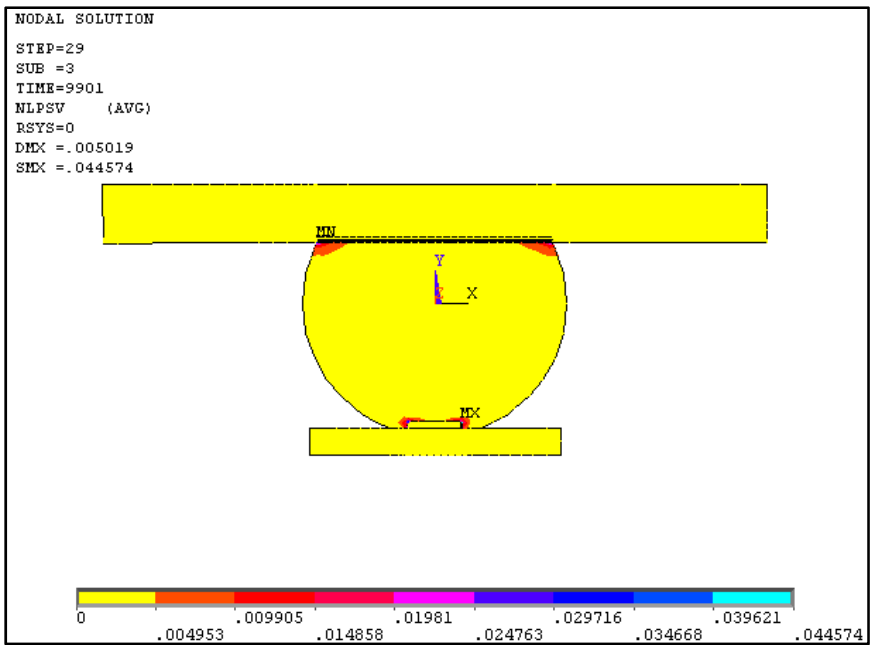

Figure 5-21 Backward compatible assembly, 1.0mm diameter, Cycle 2, properly mixed solder ball

5.2.4 PROPERLY MIXED BY CYCLE

5.2.4.1 CYCLE 1 – 0.5MM VS 0.75MM VS 1.0MM BALLS

All three solder balls show the areas around the Cu pads as having the highest energy density. Results show that the energy density, and its maximum value, increases from the 0.5mm ball to the 0.75mm ball but decreases from the 0.75mm ball to the 1.0mm ball, to the point where the energy density for the 1.0mm solder ball is less than that for the 0.5mm solder ball. When considering the affected areas it can be seen that they decrease as the size of the solder ball increases. Thus, a larger portion of the 0.5mm ball is affected in relation to the ball's size when compared to the affected area of the

1.0mm ball in relation to its size. In all three cases the maximum values of energy density were concentrated along the Cu pads, pointing to these locations as the most critical for reliability.

5.2.4.2 CYCLE 2 – 0.5MM VS 0.75MM VS 1.0MM BALLS

All three solder balls show the areas around the Cu pads as having the highest energy density. Results show that the energy density, and its maximum value, increases from the 0.5mm ball to the 0.75mm ball but decreases from the 0.75mm ball to the 1.0mm ball, to the point where the energy density for the 1.0mm solder ball is less than that for the 0.5mm solder ball. When considering the affected areas it can be seen that they decrease as the size of the solder ball increases. Thus, a larger portion of the 0.5mm ball is affected in relation to the ball's size when compared to the affected area of the 1.0mm ball in relation to its size. In all three cases the maximum values of energy density were concentrated along the Cu pads, pointing to these locations as the most critical for reliability

5.2.4.3 PROPERLY MIXED GLOBAL RESULTS

Figure 5-22 shows a plot with the results for all three solder ball geometries under each of the two thermal cycles. The solder balls subjected to cycle 2 show an

acceleration factor of 1.4 over the solder balls subjected to cycle 1 for all three geometries. The case with the highest energy density corresponds to the 0.75mm solder ball subjected to cycle 2 and the case with the lowest energy density corresponds to the 1.0mm solder ball subjected to cycle 1.

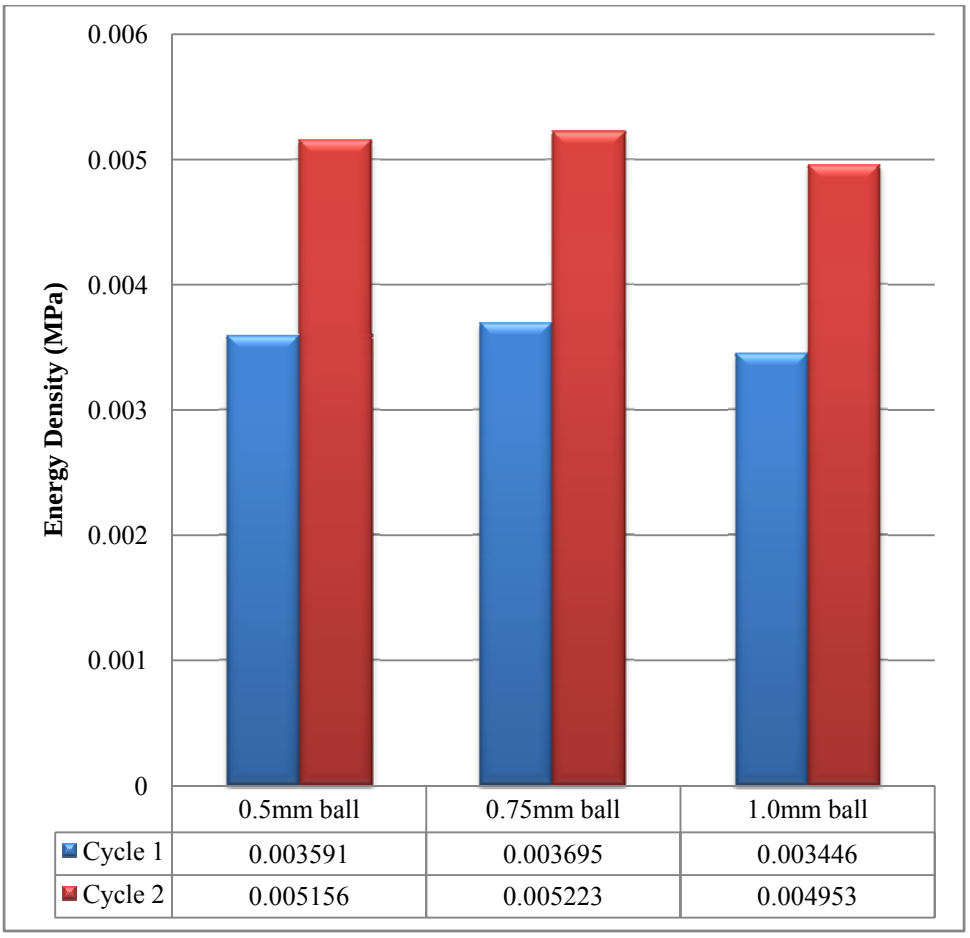

Figure 5-22 Energy Density Results for Properly Mixed Backward Compatible Assemblies

5.2.5 BACKWARD COMPATIBLE GLOBAL RESULTS

Figure 5-23 shows a plot with the results for all six backward compatible solder ball geometries under each of the two thermal cycles. The solder balls subjected to cycle 2 show an acceleration factor of 1.4 over the solder balls subjected to cycle 1 for all six geometries. In comparing the solder balls to each other in terms of size the plot shows that the smallest of the three, the 0.5mm ball, has the lowest energy density when properly mixed and the lowest energy density when improperly mixed. Of the two cases the improperly mixed one showed lower energy density.

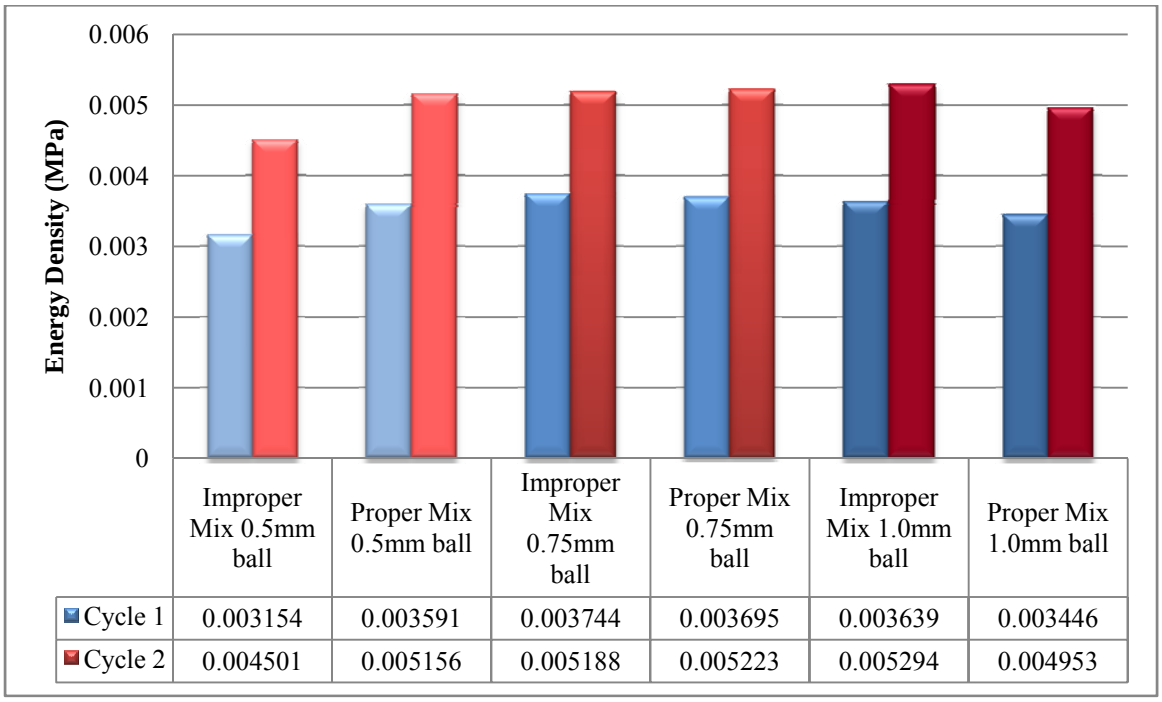

	Improper Mix 0.5mm ball	Proper Mix 0.5mm ball	Improper Mix 0.75mm ball	Proper Mix 0.75mm ball	Improper Mix 1.0mm ball	Proper Mix 1.0mm ball
Cycle 1	0.003154	0.003591	0.003744	0.003695	0.003639	0.003446
Cycle 2	0.004501	0.005156	0.005188	0.005223	0.005294	0.004953

Figure 5-23 Energy Density Results for All Backward Compatible Assemblies

5.3 RE-BALLED ASSEMBLY

5.3.1 RE-BALLED BY DIAMETER

5.3.1.1 0.5MM BALLS – CYCLE 1 VS CYCLE 2

The 0.5mm re-balled solder balls subjected to cycle 1 and cycle 2 showed a similar affected area, mostly just at the upper and bottom corners of the balls. The energy density in the case of cycle 1 is 0.010491MPa. In the case of cycle 2 the corresponding value is 0.015159MPa. The maximum energy density for cycle 1 is 0.094418MPa and 0.136431MPa for cycle 2. Thus, the 0.5mm re-balled solder ball subjected to cycle 2 has higher energy density than the same solder ball subjected to cycle 1.

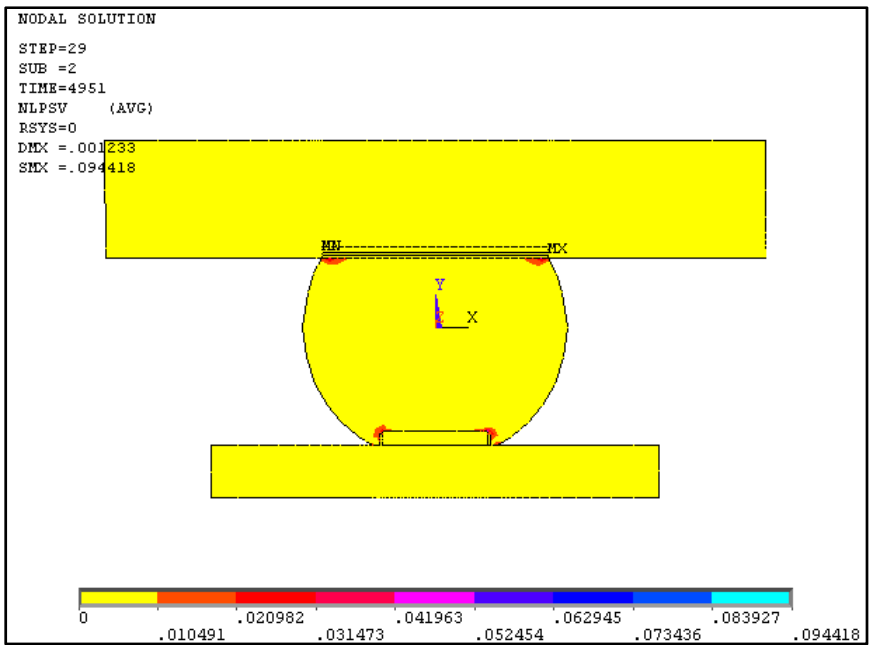

Figure 5-24 Re-balled assembly, 0.5mm diameter, Cycle 1

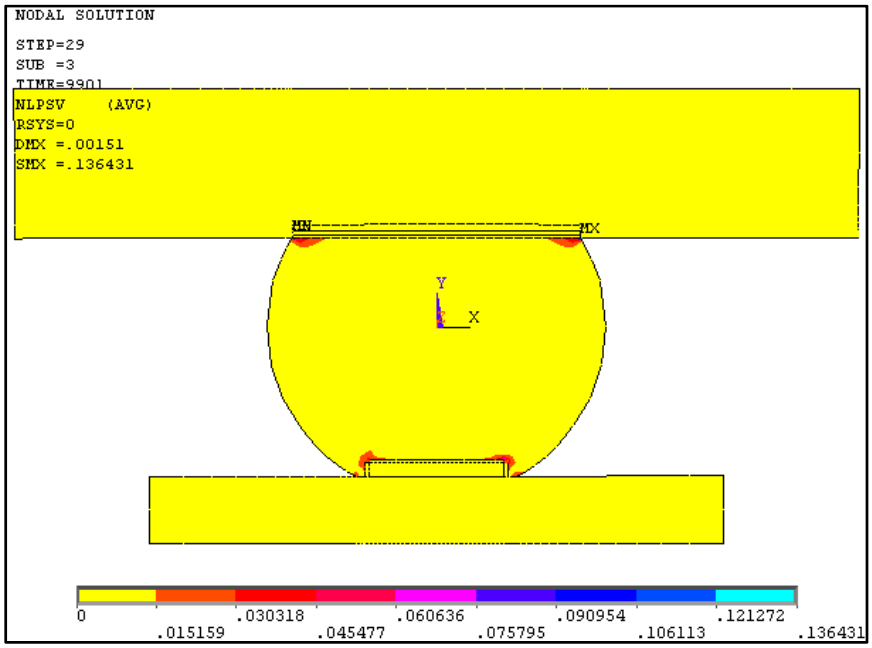

Figure 5-25 Re-balled assembly, 0.5mm diameter, Cycle 2

5.3.1.2 0.75MM BALLS – CYCLE 1 VS CYCLE 2

The 0.75mm re-balled solder balls subjected to cycle 1 and cycle 2 showed a similar affected area, mostly just at the upper and bottom corners of the balls. The energy density in the case of cycle 1 is 0.009814MPa. In the case of cycle 2 the corresponding value is 0.013716MPa. The maximum energy density for cycle 1 is 0.088326MPa and 0.123443MPa for cycle 2. Thus, the 0.75mm re-balled solder ball subjected to cycle 2 has higher energy density than the same solder ball subjected to cycle 1.

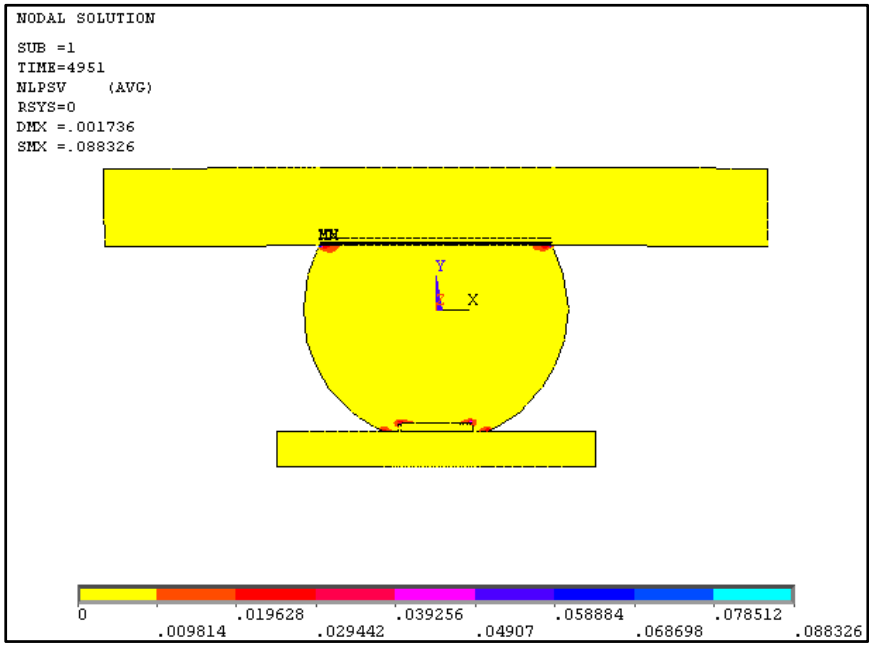

Figure 5-26 Re-balled assembly, 0.75mm diameter, Cycle 1

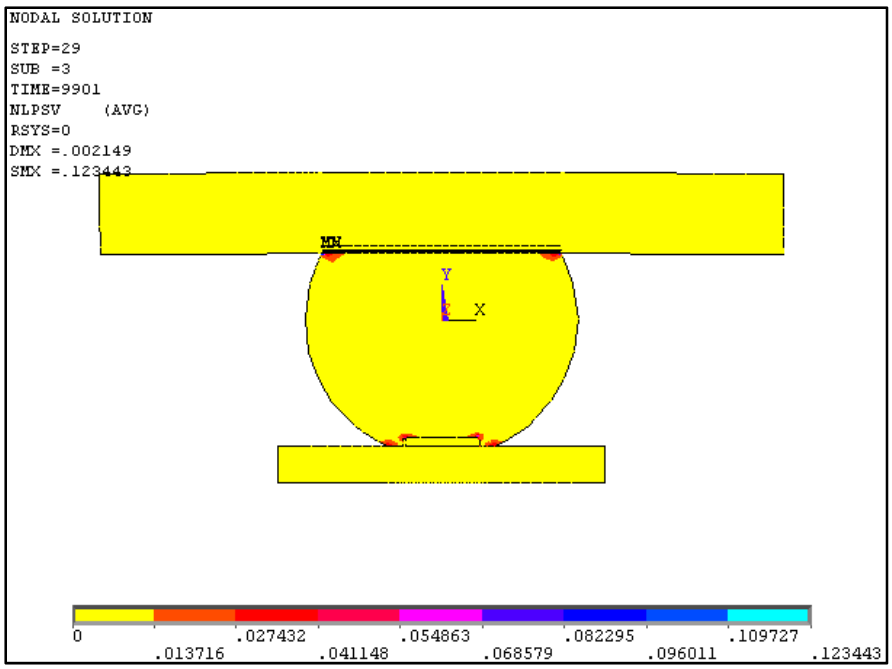

Figure 5-27 Re-balled assembly, 0.75mm diameter, Cycle 2

5.3.1.3 1.0MM BALLS – CYCLE 1 VS CYCLE 2

The 0.5mm re-balled solder balls subjected to cycle 1 and cycle 2 showed a similar affected area, mostly just at the upper and bottom corners of the balls. The energy density in the case of cycle 1 is 0.009498MPa. In the case of cycle 2 the corresponding value is 0.013367MPa. The maximum energy density for cycle 1 is 0.08548MPa and 0.1203MPa for cycle 2. Thus, the 1.0mm re-balled solder ball subjected to cycle 2 has higher energy density than the same solder ball subjected to cycle 1.

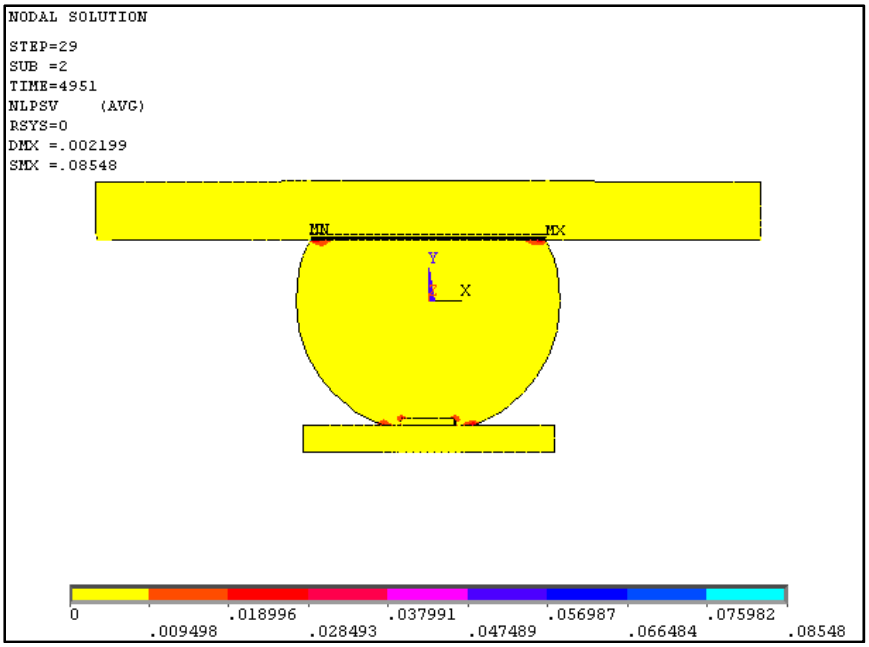

Figure 5-28 Re-balled assembly, 1.0mm diameter, Cycle 1

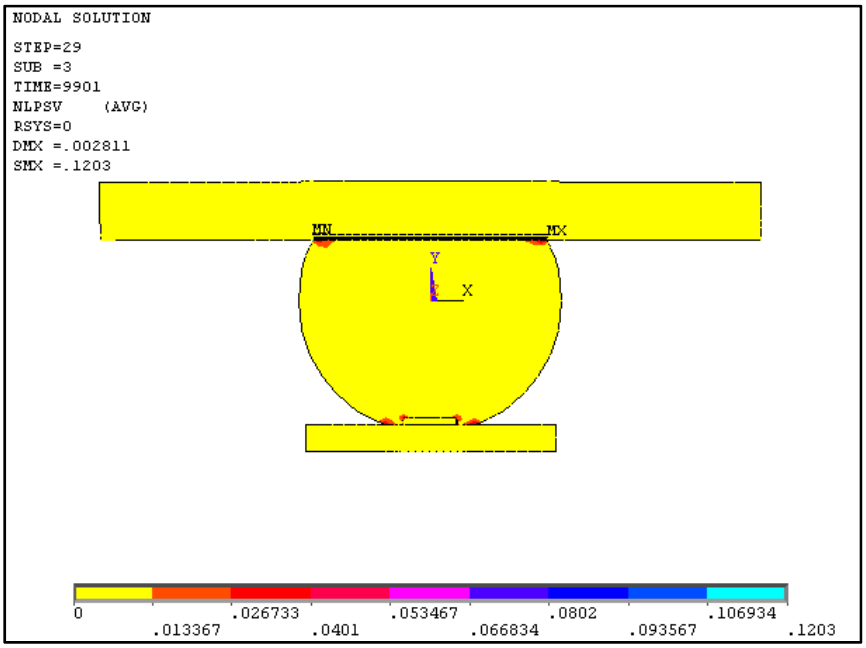

Figure 5-29 Re-balled assembly, 1.0mm diameter, Cycle 2

5.3.2 RE-BALLED BY CYCLE

5.3.2.1 CYCLE 1 – 0.5MM VS 0.75MM VS 1.0MM BALLS

The three solder balls present similar affected areas relative to the size of the specific solder ball. More specifically, all three balls show the energy density being the highest toward the corners of the balls. The corresponding values of energy density for the solder balls are 0.010491MPa for the 0.5mm ball, 0.009814MPa for the 0.75mm ball and 0.009498MPa for the 1.0mm ball. Thus, results show that the energy density, and its maximum value, decreases as the size of the solder ball increases. In all three cases the maximum values of energy density were concentrated along the Cu pads, pointing to these locations as the most critical for reliability.

5.3.2.2 CYCLE 2 – 0.5MM VS 0.75MM VS 1.0MM BALLS

The three solder balls present similar affected areas relative to the size of the specific solder ball. More specifically, all three balls show the energy density being the highest toward the corners of the balls. The corresponding values of energy density for the solder balls are 0.015159MPa for the 0.5mm ball, 0.013716MPa for the 0.75mm ball and 0.013367MPa for the 1.0mm ball. Thus, results show that the energy density, and its maximum value, decreases as the size of the solder ball increases. In all three cases the

maximum values of energy density were concentrated along the Cu pads, pointing to these locations as the most critical for reliability.

5.3.3 RE-BALLED GLOBAL RESULTS

Figure 5-30 shows a plot with the results for all three solder ball geometries under each of the two thermal cycles. The solder balls subjected to cycle 2 show an acceleration factor of 1.4 over the solder balls subjected to cycle 1. In addition, all cases show the energy density decreasing with increasing diameter. In summary, the case with the highest energy density corresponds to the 0.5mm solder ball subjected to cycle 2 and the case with the lowest energy density corresponds to the 1.0mm solder ball subjected to cycle 1.

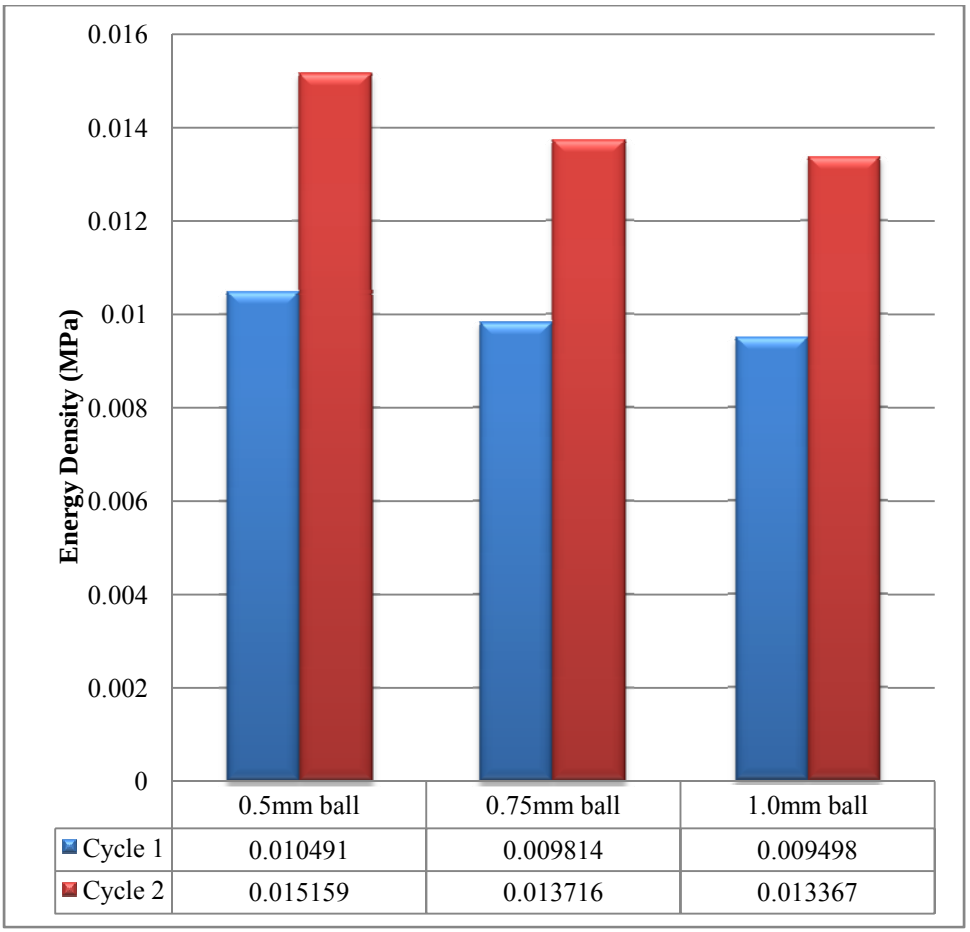

Figure 5-30 Energy Density Results for Re-Balled Assemblies

5.4 BACKWARD COMPATIBLE ASSEMBLY VS RE-BALLED ASSEMBLY

Figure 5-31 shows a plot with the results for all solder ball geometries simulated under each of the two thermal cycles of interest. The plot shows that the family of re-balled assemblies has greater energy density than the family of backward compatible assemblies. Under this consideration the family of backward compatible assemblies

shows similar energy density for the respective cycles, being lower than that of the re-balled family of solder balls for all cases.

Traditional operations on electronics manufacturing floors limit the existence of true properly mixed backward compatible assemblies. Even with strict controls the most common backward compatible assembly available to aerospace manufacturers are improperly mixed, making the properly mixed assemblies somewhat of an ideal goal. This serves as grounds for looking closely at the results for the improperly mixed assemblies in comparison to the new manufacturing trend of re-balling. As can be seen in Figure 5-31 the re-balled assemblies accumulate greater energy density than both backward compatible assemblies, including the improperly mixed one. This gives aerospace manufacturers indication of the possible reliability issues they could be facing due to the new re-balling trend on their manufacturing floors.

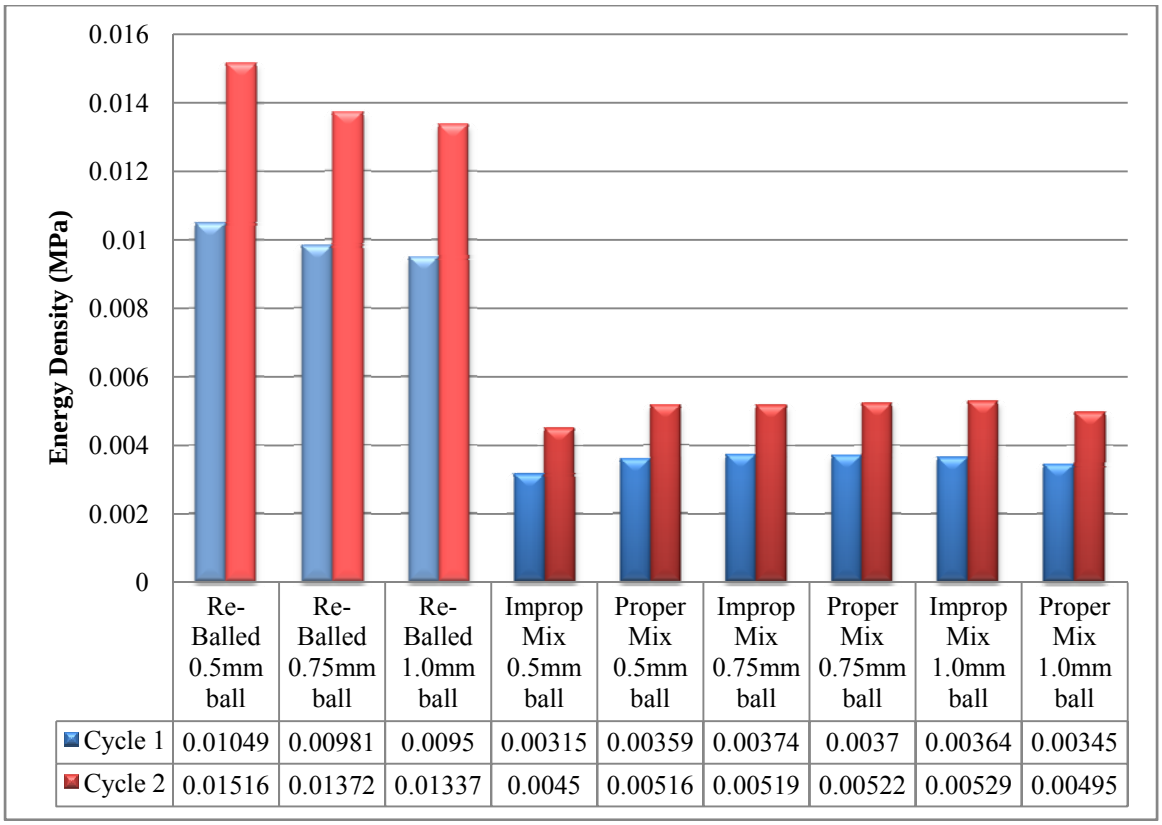

	Re-Balled 0.5mm ball	Re-Balled 0.75mm ball	Re-Balled 1.0mm ball	Improp Mix 0.5mm ball	Proper Mix 0.5mm ball	Improp Mix 0.75mm ball	Proper Mix 0.75mm ball	Improp Mix 1.0mm ball	Proper Mix 1.0mm ball
Cycle 1	0.01049	0.00981	0.0095	0.00315	0.00359	0.00374	0.0037	0.00364	0.00345
Cycle 2	0.01516	0.01372	0.01337	0.0045	0.00516	0.00519	0.00522	0.00529	0.00495

Figure 5-31 Energy Density Results for Re-Balled and Backward Compatible Assemblies

6 CONCLUSION

This study compared the behavior of backward compatible SnAgCu solder balls versus re-balled SnPb solder balls with eutectic solder paste under thermal cycling loading through an extensive detailed two-dimensional viscoplastic finite element analysis. The major outputs of this study were thermal cycling test results and inelastic energy density accumulation, outputs that showed that the thermo-mechanical durability model of the backward compatible Pb-free solders outperformed re-balled SnPb.

The models for two unconventional but possible scenarios were used to predict thermo-mechanical durability of SnAgCu balls soldered with SnPb paste under accelerated life testing. The results show that properly mixed backward compatible solder balls have similar maximum energy than improperly mixed backward compatible solder balls. However, inelastic energy density per cycle averaged over damage volume is higher across the bulk of the solder ball for improperly mixed backward compatible solder balls when compared to properly mixed backward compatible solder balls. The

model for another scenario was used to predict thermo-mechanical durability of re-balled SnPb balls soldered with SnPb paste under accelerated life testing. The results show that the re-balled solder balls have higher maximum energy than all backward compatible solder balls. Thus, backward compatible assemblies with commercially available SnAgCu components showed less energy density than re-balled SnPb components.

The results of this study permit extrapolation of laboratory results to field life predictions and to explore the design of accelerated re-balled or backward compatible BGA tests that relate better to application-specific usage environments. For example, high-frequency thermal changes from usage environments may be simulated with the models presented in this study to assess the damage and select a test thermal cycle that will accelerate the same type of damage. The damage assessment methodology outlined in this study appropriately recognizes the significant differences in the energy states achieved under test loads and those energy states that may be expected in the use environments. It may therefore provide a scientific way to extrapolate accelerated test results to field predictions through quantitative acceleration factors.

FEA in three dimensions is recommended for future work, as well as the modification of the constitutive models employed to better reflect the behavior of the materials as new experimental data in this field emerges. Further validation of FEA results with experiments using assemblies as described in this study may also be explored in the future.

7 APPENDIX – LEAD AND LEGISLATION

7.1 LEAD

Pb is a heavy, bluish-gray metal that occurs naturally in the Earth's crust.[23] However, it is rarely found naturally as a metal. It is usually found combined with two or more other elements to form Pb compounds and is commonly mined in the states of Alaska and Missouri. Metallic Pb is resistant to corrosion and is easily molded and shaped. Pb and Pb alloys are commonly found in pipes, storage batteries, weights, shot and ammunition, cable covers, and sheets used as radiation shields. Pb compounds are used in automotive batteries, as a pigment in paints, dyes and ceramic glazes, and even as a pesticide for fruit orchards dating before the 1950's. Pb has been proven to be harmful to health, so the amount of Pb used in these products has been reduced in recent years.

Tetraethyl Pb and tetramethyl Pb were once used in the United States as gasoline additives to increase octane rating. However, their use was phased out in the United

States in the 1980s, and Pb was banned for use in gasoline for motor vehicles beginning January 1, 1996. It is worth noting that Pb and its compounds are still used in several developing countries.

The 2007 Comprehensive Environmental Response, Compensation, and Liability Act (CERCLA) Priority List of Hazardous Substances lists Pb as the number 2 most important toxic substance in the United states, just after arsenic.[24] The CERCLA requires the Agency for Toxic Substances and Disease Registry (ATSDR) of the Department of Health and Human Services (DHHS) and the Environmental Protection Agency (EPA) to prepare a list, in order of priority, of substances that are most commonly found in the US. These substances are determined to pose the most significant potential threat to human health due to their known or suspected toxicity and potential for human exposure. It should be noted that this priority list is not a list of "most toxic" substances, but rather a prioritization of substances based on a combination of their frequency, toxicity, and potential for human exposure.

7.1.1 LEAD AND THE ENVIRONMENT

Pb occurs naturally in the environment. However, most of the high concentration levels found throughout the environment come as a direct result of human activities. Environmental levels of Pb have increased more than 1,000-fold over the past three centuries as a result of human activity. The greatest increase occurred between the years

1950 and 2000, and has been directly linked to the increase of Pb additives in gasoline. This use, in addition to manufacturing processes that use Pb, mining for Pb and waste products has Pb to this dramatic increase. Since EPA banned the use of leaded gasoline for highway transportation in 1996, the amount of Pb released into the air has decreased further. Yet Pb in the air is still common, and rainwater removes it from the air and deposits it into soil and water resources. Other than rainwater, sources of Pb in soil and bodies of water include the chipping of lead-based paint from buildings, bridges, and other structures and runoff water from leaded waste in landfills. Landfills may contain waste from Pb ore mining, ammunition manufacturing, or other industrial activities such as battery production, and the disposal of lead-containing products by consumers.

7.1.2 LEAD AND HEALTH

Pb is commonly found in soil especially near roadways, older houses, old orchards, mining areas, industrial sites, near power plants, incinerators, landfills, and hazardous waste sites. People living near hazardous waste sites may be exposed to Pb and chemicals that contain Pb by breathing air, drinking water, eating foods, or swallowing dust or dirt that contain Pb. Canned foods may contain small amounts of Pb, especially if the canned food is imported from outside the United States. This is primarily due to the use of leaded solder used in the manufacturing process. However, since Pb solder is no longer used in cans in the US, very little Pb is found in food. Leafy fresh vegetables grown in lead-containing soils may have lead-containing dust on them.

Pb may also enter foods if they are put into improperly glazed pottery or ceramic dishes and from leaded-crystal glassware. Children may be exposed to Pb by hand-to-mouth contact after exposure to Pb containing soil or dust. Skin contact with dust and dirt containing Pb occurs frequently, especially when handling inexpensive jewelry, some cosmetics, hair dyes, children's toys containing Pb paint and children's books published with ink containing Pb, reason for which US public libraries are currently removing children's books published before 1985 from their shelves.[25]

Once Pb gets into your lungs, it goes quickly to other parts of the body in your blood. Larger particles that are too large to get into your lungs can be coughed up and swallowed. Shortly after Pb gets into your body, it travels in the blood to the "soft tissues" and organs (such as the liver, kidneys, lungs, brain, spleen, muscles, and heart). Once it is taken in and distributed to your organs, the Pb that is not stored in your bones leaves your body in your urine or your feces. Under conditions of continued exposure, not all of the Pb that enters the body will be eliminated, and this may result in accumulation of Pb in body tissues, especially bone. The main target for Pb toxicity is the nervous system, both in adults and children. Pb exposure may cause weakness in fingers, wrists, or ankles, increases in blood pressure, anemia, severe damage to the brain and kidneys, and death. The DHHS has determined that Pb and Pb compounds are reasonably anticipated to be human carcinogens, and the EPA has determined that Pb is a probable human carcinogen.

7.2 LEGISLATION BANNING USE OF LEAD

7.2.1 RESTRICTION OF HAZARDOUS SUBSTANCES

The Restriction of Hazardous Substances directive (RoHS) is easily the most important piece of legislation affecting electronic products today. This directive of the European Union requires that certain products placed in the European market after July 1, 2006 must not contain hazardous substances in amounts greater than the established. Table 7-1 summarizes these substances and the allowable levels of each.

Table 7-1 Maximum Allowable Concentrations of RoHS Restricted Substances

Restricted Substance	Maximum Concentration Value
Lead	0.1% by weight
Mercury	0.1% by weight
Hexavalent chromium	0.1% by weight
Cadmium	0.01% by weight
Polybrominated biphenyls	0.1% by weight
Polybrominated diphenyl ethers	0.1% by weight

The purpose of this directive is to approximate the laws of the Member States of the European Union on the restrictions of the use of hazardous substances in electrical and electronic equipment and to contribute to the protection of human health and the

environmentally sound recovery and disposal of waste electrical and electronic equipment.

Under the RoHS, electrical and electronic equipment is defined as "equipment which is dependent on electric currents or electromagnetic fields in order to work properly and equipment for the generation, transfer and measurement of such currents". Member States shall ensure that, from 1 July 2006 onward, new electrical and electronic equipment put on the market does not contain lead, mercury, cadmium, hexavalent chromium, polybrominated biphenyls or polybrominated diphenyl ethers in amounts greater than those established in Table 7-1.

7.2.2 OTHER LEGISLATION

The RoHS directive is not the only piece of legislation currently banning the use of Pb or regulating its disposal. The European Union has also implemented the Waste of Electrical and Electronic Equipment (WEEE) directive and other nations are taking steps in the same direction.

WEEE is EU legislation restricting the use of hazardous substances in electrical and electric equipment and promoting the collection and recycling of such equipment has been in force since February 2003.[26] The legislation provides for the creation of collection schemes where consumers return their used e-waste free of charge. The

objective of these schemes is to increase the recycling and/or re-use of such products. It also requires heavy metals such as lead, mercury, cadmium, and chromium and flame retardants such as polybrominated biphenyls or polybrominated diphenyl ethers to be substituted by safer alternatives.[27] In Member States where the consumption of electrical and electronic equipment is widespread the most ambitious targets will be set. In the same manner, smaller consumers of electronic equipment will have less ambitious targets.

On February 28, 2006, the Chinese Ministry of Information Industry promulgated China's requirements for the Management Methods for Controlling Pollution Caused by Electronic Information Products Regulation.[28] The legislation came into effect in November, 2006. These requirements are referred to as the Chinese version of the Restriction of Hazardous Substances (RoHS) and applies to what they refer to as Electronic Information Products. The Chinese directive is similar to the RoHS in that they recognize the same six hazardous substances and the same maximum concentration levels as the European Union. The document also defines requirements for product labeling and hazardous substance level disclosure.

Japan and South Korea have taken steps toward the management of hazardous substances and its waste as well.[29] While they have not issued formal legislation on the subject, they have taken steps toward assessing recyclability of products, labeling products containing hazardous substances and substituting hazardous substances for less toxic ones whenever possible.

Western countries in North and South America have not taken steps toward the restriction of hazardous substances and effective waste management in the way that the European Union and Eastern nations like China, Japan and South Korea have. It is generally expected that the United States, Canada, Mexico and South American nations will transition toward this type of legislation, but this is still not in the horizon.

8 REFERENCES

[1] United States Environmental Protection Agency Lead Awareness Program (2009) Lead in Paint, Dust and Soil. In: http://www.epa.gov/lead/index.html

[2] United States Environmental Protection Agency Pollution Prevention and Toxics (2009) Laws, Regulations and Statutes. In: http://www.epa.gov/opptintr/pubs/laws.htm

[3] United States Department of Health and Human Services (2009) Toxic Substances Portal CAS ID #: 007439-92-1. In: , Agency for Toxic Substances and Disease Registry, Atlanta, GA

[4] The European Parliament and the Council of the European Union (2003) Directive 2002/95/EC of the European Parliament and of the Council of 27 January 2003 on the Restriction of the Use of Certain Hazardous Substances in Electrical and Electronic Equipment. In: Official Journal of the European Union, Brussels, pp L 37/19 - L 37/23

[5] Pinsky D, Rafanelli A, Condra L, Amick P, Anderson V (2008) How the Aerospace Industry is Facing the Lead-free Challenge. White Paper: Prepared by the Lead-free in Aerospace Project- Working Group

[6] Pan J, Bath J, Zhou X, Willie D (2007) Backward and Forward Compatibility. In: Bath, J (Ed.), Lead –Free Soldering, pp 173-197. Springer Science + Business Media, LLC, New York.

[7] Bath J, Sethuraman S, Zhou X, Willie D, Hyland K, Newman K, Hu L, Love D, Reynolds H, Kochi K, Chiang D, Chin V, Teng S, Ahmed M, Henshall G, Schroeder V, Nguyen Q, Maheswari A, Lee MJ, Clech J-P, Cannis J, Lau J, Gibson C (2005) Reliability Evaluation of Lead-free SnAgCu PBGA676 Components using Tin-Lead and Lead-free SnAgCu Solder Paste. In: Proceedings of 2005 SMTA International, Chicago, IL, pp 891-901.

[8] Nandagopal B, Chiang D, Teng S, Thune P, Anderson L, Jay R, Bath J (2005) Study on Assembly, Rework, Microstructures and Mechanical Strength of Backward Compatible Assembly. In: Proceedings of 2005 SMTA International, Chicago, IL, pp 861-870.

[9] National Center for Manufacturing Sciences (1997) NCMS Lead-Free Solder Project Final Report. In: Report 0401RE96, Ann Arbor, MI

[10] Morgan HS (1994) Thermomechanical Modeling of Solder Joints – Numerical Considerations. In: The Mechanics of Solder Alloy Interconnects, Chapman & Hall, New York, NY, pp 314-333

[11] Vandevelde B, Gonzalez M, Limaye P, Ratchev P, Beyne E (2006) Thermal Cycling Reliability of SnAgCu and SnPb Solder Joints: A Comparison for Several IC-Packages. In: Microelectronics Reliability 47 pp 259–265

[12] Zhang Q, Dasgupta A (2005) systematic Study on Thermo-Mechanical Durability of Pb-Free Assemblies: Experiments and FE Analysis. In: Transactions of the ASME, Journal of Electronic Packaging, Vol.127, December 2005, pp415-429.

[13] Limaye P, Vandevelde B, Labie R, Vandepitte D, Verlinden B (2008) Influence of Intermetallic Properties on Reliability of Lead-Free Flip-Chip Solder Joints. In: IEEE Transactions on Advanced Packaging, Vol.31, No.1, pp 51-57

[14] Personal conversation with member of research team of unpublished study

[15] Dally J, Lall P, Suhling J (2002) Mechanical Design of Electronic Systems - Introduction. In: Mechanical Design of Electronic Systems, College House Enterprises, Knoxville, TN, pp3-18

[16] Dally J, Lall P, Suhling J (2002) First Level Packaging – The Chip Carrier. In: Mechanical Design of Electronic Systems, College House Enterprises, Knoxville, TN, pp 109-111

[17] Xu Y, Liang L, Liu Y (2005) Models Correlation and Comparison for Solder Joint Reliability. In: IEEE 6th International Conference on Thermal, Mechanical, Multiphysics Simulation and Experiments in Micro-electronics and Micro-Systems, pp423-429

[18] Darveaux R, Banerji K (2002) Constitutive relations for tin-based solder joints. In: IEEE Trans Compon, Hybr Manuf Technol 1992;15(6): 1013–24

[19] Wiese S, Meusel E, Wolter KJ, microstructural dependence of constitutive properties of eutectic SnAg and SnAgCu solders. In: Proceedings of the 53rd electronic components and technology conference; 2003. p. 197–206.

[20] S. C. Tseng . R. S. Chen . C. C. Lio (2006) Stress Analysis of Lead-free Solders with Under Bump Metallurgy in a Wafer Level Chip Scale Package. In: International Journal of Advanced Manufacturing Technologies, 31:1-9

[21] Lucas JP, Rhee H, Guo F, Subramanian, KN (2003) Mechanical Properties of Intermetallic Compounds Associated with Pb-Free Solder Joints Using Nanoindentation. In: J. of Electronic Materials, Vol. 32, No. 12, pp 1375-84.

[22] Huang Z, Liu C, Conway P, R Thornson (2004) Characterisation of Intermetallics and Mechanical Behaviour in the Reaction between SnAgCu and Sn-Pb Solder Alloys. In: Proceeding of HDP, pp 52-59.

[23] United States Department of Health and Human Services (2009) Toxic Substances Portal CAS ID #: 007439-92-1. Agency for Toxic Substances and Disease Registry, Atlanta, GA

[24] United States Department of Health and Human Services in Cooperation with United States Environmental Protection Agency (2007) CERCLA Priority List of Hazardous Substances that will be the Subject Toxicological Profiles and Support Document. Agency for Toxic Substances and Disease Registry, Atlanta, GA

[25] Lee L (2009) New Law on Lead Exposure Causes Dust-Up over Children's Books, Associated Press, Cable News Network, March 17 2009

[26] EUROPA (2009) Waste Electrical and Electronic Equipment. In: EUROPA, the Portal of the European Union, http://ec.europa.eu/environment/waste/weee/index_en.htm

[27] The European Parliament and the Council of the European Union (2003) Directive 2002/96/EC OF THE EUROPEAN PARLIAMENT AND OF THE COUNCIL of 27 January 2003 on waste electrical and electronic equipment (WEEE)

[28] Ministry of Information Industry of the People's Republic of China (2006) Requirements for Concentration Limits for Certain Hazardous Substances in Electronic Information Products. In: Standard of the Electronics Industry of the People's Republic of China SJ/T 11363 – 2006

[29] Shepherd, J (2007) Lead Restrictions and Other Regulatory Influences on the Electronics Industry In: Bath, J (Ed.), Lead –Free Soldering, pp 15-17. Springer Science + Business Media, LLC, New York.